Applied Energy 231 (2018) 1285–1306

Contents lists available at ScienceDirect

Applied Energy

journal homepage: www.elsevier.com/locate/apenergy

A comparison of storage systems in neighbourhood decentralized energy system applications from 2015 to 2050

Portia Murray[a,b,*], Kristina Orehounig[a,b], David Grosspietsch[c], Jan Carmeliet[a]

[a] Chair of Building Physics ,D-MAVT, Swiss Federal Institute of Technology, Zürich, Switzerland
[b] Urban Energy Systems Laboratory, Swiss Federal Laboratories for Materials Science and Technology, Empa, Dübendorf, Switzerland
[c] Group for Sustainability and Technology, D-MTEC, Swiss Federal Institute of Technology, Zürich, Switzerland

HIGHLIGHTS

- Long-term (hydrogen) and short-term (batteries and thermal) storage are evaluated.
- Multi-objective optimization platform minimizes both costs and CO_2 emissions.
- Optimal solutions for neighbourhoods are compared against national CO_2 targets.
- Three future scenarios between 2015 and 2050 are developed predict future outcomes.
- Two test decentralized neighbourhoods (one urban and one rural) are compared.

GRAPHICAL ABSTRACT

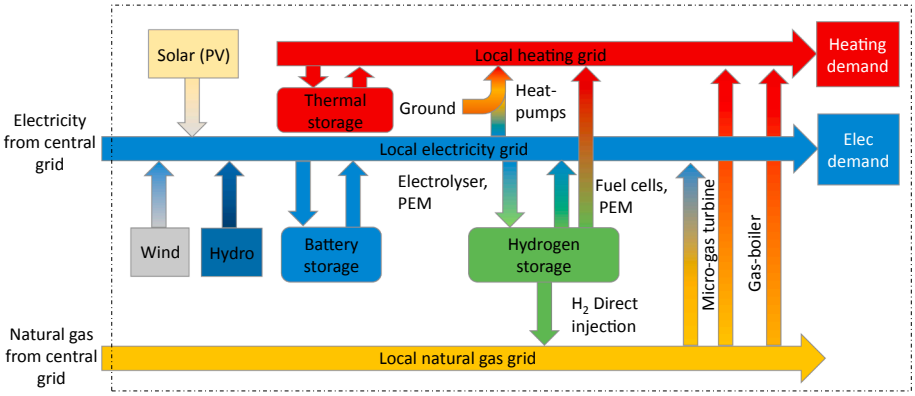

ARTICLE INFO

Keywords:
Decentralized energy systems
Power-to-hydrogen
Multi-objective optimization
Renewable energy sources
Storage technologies

ABSTRACT

The potential of both long-term (hydrogen storage) and short-term (batteries and thermal) storage systems in decentralized neighbourhoods are assessed using a multi-objective optimization approach that minimizes both costs and CO_2 emissions. A method is developed, which evaluates the performance of long and short-term storage systems in the future based on multi-objective optimization. More specifically, hydrogen storage is investigated for its future potential to be used as a long-term storage in a decentralized context and it is compared with short-term storage systems such as batteries and thermal storage. In order to analyze potential future developments, a scenario approach is deployed based on the Intergovernmental Panel of Climate Change's 'Special Report on Emissions Scenarios'. Three future scenarios are defined and simulated for the years of 2015, 2020, 2035, and 2050 for both a rural and an urban neighbourhood in Switzerland. Based on the scenarios, the energy demand and renewable potential projections until 2050 are simulated including retrofitted buildings and renewable potential in the neighbourhoods. The Pareto front of solutions is then benchmarked against national carbon and energy targets from 2020 until 2050. In addition, a range of parameter assumptions (e.g., for economic variables, policy changes, environmental conditions) are used in each scenario to incorporate uncertainty into the analysis. The long-term storage potential of hydrogen, in particular, is evaluated for its capability to shift renewable surpluses in summer towards demand later in the year. From the results, it is predicted that neighbourhoods with high renewable surpluses (i.e., in rural settings) should consider the advantages of a hydrogen storage system from 2035 to 2050. For neighbourhoods with low surpluses, short-term battery and thermal storage systems are predicted to be sufficient for load shifting. It is also observed that a high feed-in

* Corresponding author at: Chair of Building Physics, D-MAVT, Swiss Federal Institute of Technology, Zürich, Switzerland.
E-mail address: murrayp@ethz.ch (P. Murray).

https://doi.org/10.1016/j.apenergy.2018.08.106
Received 24 May 2018; Received in revised form 27 July 2018; Accepted 18 August 2018
Available online 05 October 2018
0306-2619/

remuneration undermines on-site consumption, thus resulting in lower levels of storage deployment due the selling of production back to the centralized electricity grid. Lastly, it is concluded that both an increase in renewable technology deployment and in the retrofit rate of buildings will both be required to meet energy targets for the two case studies. As the renewable potential in urban contexts is limited, it is particularly important for older building stock to be retrofitted at a high rate (more than 2% of buildings per year) in order to reduce the end energy demand of the buildings. The approach used in this article is widely applicable both in spatial scope (e.g., other decentralized energy systems, geographies) and temporal scope (e.g., different years, scenarios) and allows for an optimization with a range of objective functions, thus making it an effective approach to identify the renewable and storage technologies that can contribute to most of the decarbonization of the building stock in the future.

Nomenclature

CHP	combined heat and power
CM	conventional markets
CRF	capital recovery factor
DES	decentralized energy systems
DI	direct injection
EC	electrolyzer
FC	fuel cell
FIT	feed-in tariff
IPCC	intergovernmental panel
GB	gas boilers
GIS	geographical information system
GSD	global sustainable development
GWR	buildings and apartments registry
H2S	compressed hydrogen storage tank
LCOE	levelized cost of energy
LCO2	levelized CO2 emissions
MILP	mixed integer linear programming
MGT	micro-gas turbine
OMF	fixed operation and maintenance
OMV	variable operation
PEM	polymer electrolyte membrane
P2H	power to hydrogen
PWA	piecewise affine
PV	photovoltaics
RES	renewable energy sources
RSD	regional sustainable development
TES	thermal energy storage

1. Introduction

In order to support energy self-reliance within countries, decrease greenhouse gas emissions, and reduce dependence of a declining fossil fuel supply, renewable energy sources (RES) are planned to replace a large percentage of fossil fuel electricity generation by 2050. With the replacement of centralized plants with decentralized solar photovoltaics (PV) or wind turbines, the energy future may rely on partial shifts from centralized energy generation to distributed energy generation that is based around neighbourhoods of prosumers in decentralized energy systems (DES) [1].

The major drawback of RES is that they are non-dispatchable, thus their output generation fluctuates stochastically over time with associated weather conditions (i.e., solar radiation or wind velocities), resulting in a temporal mismatch of supply and demand. Currently, this temporal mismatch is managed by exporting excess renewable production to the grid or curtailing renewable production and then importing electricity from the grid when demand is not met by renewable energy supply. However, as the fraction of renewables in our electricity grid increases, this temporal mismatch will become more severe.

1.1. Motivation

In order to allow shifting of non-dispatchable loads, energy storage is required [2]. Energy storage comes in many different forms, with the most prominent technologies being batteries, pumped-hydro storage, and thermal energy storage. A technological split into short and long-term storage represents a common solution [3]. Shifting demand over longer periods of time is important, as there is often not only a day-to-night mismatch of renewable energy and demand but also a seasonal mismatch as RES are more plentiful in summer and energy demand of buildings is higher in the winter in heating dominated climates.

A promising long-term storage option is hydrogen storage or power-to-hydrogen (P2H). P2H refers to the use of an electrical current, in this case from surplus renewable electricity production, to split water via electrolysis into hydrogen and oxygen. The hydrogen can be stored in compressed tanks or metal hydride storage, used to run fuel cells, can be directly injected into the natural gas grid up to certain concentration limitations, or converted to methane via methanation and used as a substitute for natural gas [4]. This technology can be installed in both a centralized or decentralized context and is not ideally considered to have time dependent losses [5].

There are two major disadvantages currently associated with P2H: the technology is expensive and it typically has low round-trip efficiencies. Current research into hydrogen technologies, such as fuel cells, hydrogen storage, and electrolysis, are constantly improving both equipment costs and efficiencies. In addition, the need for energy storage should increase with the predicted phase-out of feed-in tariffs and increasing implementation of RES [6]. In order to assess the changes in these model parameters over time, a scenario based approach, looking at a time horizon from 2015 to 2050, is developed to assess the optimal technology combination over time to investigate if P2H is predicted to become more cost effective on the decentralized level in the future.

In order to predict future parameters (e.g., technology costs, fuel prices, feed-in tariffs, efficiencies, etc.) that are required in an energy optimization model, there are a large amount of assumptions and uncertainty that goes into parameter selection. In order to deal with uncertainty, a scenario based approach for potential future development is used. These future scenarios are based on a report from the Intergovernmental Panel on Climate Change's (IPCC) 'Special Report on Emission Scenarios' [7]. This report contains descriptions of several possible energy futures including projections and storylines on which model assumptions can be based. They provide a framework for the development of scenarios covering assumptions on the uncertain parameters.

1.2. Literature review

There is a wide array of literature dedicated to the design and analysis of DES using optimization. First, due to the large number of publications on DES optimization, papers that have a focus on the hydrogen economy and have applications for stationary building and

mobility demands are considered. Second, papers that include future scenarios or optimization horizons for long-term energy planning are presented. Finally, the research gap is derived and the focus of this study is outlined. Several of the publications on DES are based on optimization and the Energy Hub concept that was defined by Geidl et al. in 2006 [8]. In this definition paper, Energy Hubs are described as a "system, where multiple energy carriers can be converted, conditioned, and stored to satisfy a set of demands". Technologies are defined as energy converters that can transfer energy from one carrier to another at a certain efficiency. In Geidl et al. (2006) [8], hydrogen is included as an energy carrier in optimal power flow of DES.

This method was then expanded by Hajmiragha et al. (2017) [9]. The authors further developed an optimal power flow model with additional hydrogen energy considerations, such as fuel cell vehicle charging infrastructure. Their optimization model used hydrogen converters as well as district heat, natural gas, hydrogen, and electricity. Building energy demand and fuel cell vehicle demand, in the form of hydrogen, were included in the model.

A similar method using Energy Hubs was also used by Maroufmashat et al. (2016) [10]. The authors created a mixed integer linear program (MILP) model for four pre-defined urban districts over a year of operation. The optimization included the design of hydrogen charging facilities within four urban districts.

Several other papers reviewed the design and optimization of hydrogen storage systems for applications of on-site renewable facilities, such as wind farms or large solar installations in rural areas. Zhang et al. (2017) used a genetic algorithm to design a PV-Battery-Hydrogen system using a multi-objective analysis that minimized costs and maximized self-sufficiency [11]. It was found that under pessimistic costs, batteries were a cheaper option, however under optimistic costs, hydrogen storage was competitive with batteries and performed better when accounting for grid power fluctuations. The heating energy carrier was not addressed in this system. Bernal-Augustín et al. (2010) created a techno-economical optimization of PV-Wind systems with a grid connection [12]. The model focused on power feed-into the grid and selling of hydrogen. It was found that the selling price of hydrogen would have to be high in order to recover the capital costs for the system in 10 years [12].

Similarly, Korpas et al. (2006) developed an operation planning model for a wind-hydrogen model participating in power markets. When wind electricity production was in excess, hydrogen was produced via an electrolyser and stored. Electricity was then later produced via hydrogen in fuel cell and was then sold back to the electricity grid on the spot market. Alternatively, hydrogen was also used directly for fuel cell vehicle charging [13]. They used linear optimization to determine the operational set points of an electrolyser and fuel cell using a receding horizon control strategy and participated in arbitrage to maximize profits. It was found that electricity prices must have a large variability for the fuel cell to be used, since the overall efficiency of the system is relatively low for electricity production. The authors recommended combining the scheduling model with a investment cost model and a long time horizon to estimate cost reductions and efficiency improvements over time in different power systems [13].

Petruschke et al. (2014) used a combination of a heuristic and linear optimization structure to separate the optimizations for system configuration, technology sizing, and operation for a PV-Wind-Hydrogen system on an island. This paper states that it was able to reduce simulation time due to the separation of the sizing and operations optimization which represents a multi-layer simulation approach. The paper investigated different percentages of renewable shares for the electric grid (heat demand was not considered) and found that the size of the hydrogen system was increased as the renewable share increased. Batteries and thermal storage were not considered in the model [14].

Li et al. (2017) used a bi-level optimization for a stand-alone microgrid capable of providing electric power, cooling, heating, and hydrogen demands [15]. This bi-level strategy applies a MILP to simulate the operation and a genetic algorithm to size the component decision variables. Uncertainties were taken into account using a Minimax robust optimization approach. They also considered degradation of the storage technologies in the model and found that fuel cells, batteries, and electrolysers were sized larger when degradation was accounted for. The uncertainty analysis found that higher levels of uncertainty resulted in larger sizes of storage to buffer the uncertainty in the demand and in the renewable forecasts. Lastly, Dufo-López et al. (2008) performed a triple-objective optimization for the design of a PV-wind-diesel-hydrogen-battery system in Spain using a genetic algorithm [16]. The three optimizations represented minimization of costs, minimization of emissions, and minimization of unmet demand in kWh/year. The authors found that "Due to the high costs of the hydrogen components, energy storage in most solutions is done only using batteries".

Yang et al. (2016) investigated the optimal operation of residential, commercial, and industrial prosumers in a DES and found that the active participation of the prosumers played an important role in better response to time of use electricity prices and that peak shaving could be better managed for the community as a whole. Electricity, cooling, plug-in hybrid vehicle, and heating demands were all considered in this model, however only the dispatch was optimized, as opposed to the full design and operation of the system. In addition, only short-term storage with batteries and thermal storage were considered [17].

A major shortcoming of the assessed literature, with the exception of Dufo-López et al. (2008) [16] and Zhang et al. (2017) [11], is the storage duration considered. One of the main benefits of P2H storage is its long storage cycle durations over many months, thus it is able to store seasonal variations without time dependent losses. Many of the papers discussed use the typical days method [18], or a rolling horizon method [15], to reduce the time horizon of the simulation from 365 days into a shorter horizons to reduce the computational complexity of the optimization. The typical days method does not allow for storage continuity across days as simulated days are non-consecutive thus it cannot be used to accurately assess storage durations longer than the length of the time-slices. The rolling horizon method can be used to allow for storage continuity over longer periods, as was done in Marquant et al. 2015 [19]. Marquant et al. recommended that the rolling horizon approach should be aggregated in order to consider long-term storage horizons and that it must be coupled with a genetic algorithm in order to consider simultaneous design and operation. The receding horizon method is very similar to the rolling horizon method as it uses a moving time horizon, however it is typically used for model predictive control (MPC) optimization (as shown in Korpas et al. [13]) rather than for design and planning optimization models. However the shortening of time horizon using these techniques does not sufficiently allow for accurate analysis of long-term storage design and operation and thus is limited in assessing the long-term potential of P2H. This is particularly true for case studies with large renewable potentials and high seasonal fluctuations. The most accurate method to consider long-term storage is still to use a full horizon.

Multiple studies exist that have used optimization in the context of future energy systems to identify and assess strategies for reducing emissions. In Lunz et al. (2016), a methodological approach using Germany in 2050 was used with multi-objective optimization for 29 scenarios selected from previous studies. This work focused on analysis at the national level (i.e., Germany) instead of DES at the neighbourhood or district scale [20].

In assessing future feasibility of P2H systems, the JRC-EU TIMES model [21], which used linear optimization to model future energy scenarios from a policy perspective, was applied to hydrogen technologies and power-to-gas in Sgobbi et al. (2016) [22]. In this study, the model was run for two pre-defined policy scenarios for the years of 2020, 2030, 2040, and 2050 for the EU. The results showed that hydrogen technologies were relevant for meeting long-term emission reduction targets and indicated that they might become economically feasible by 2040, particularly in the industrial sector.

In Han et al. (2017), a DES was designed for the island of Jeju in South Korea. The authors used optimization and scenarios framed as conventional energy, transitional energy, and 100% renewable energy scenarios to meet thermal, electrical, and vehicle demands on the island. Although the study is framed in scenarios, the evolution of the energy system over time is not considered [23]. In Ren and Gao (2010), a MILP model was used for the integration and evaluation of DES for a campus in Japan. The model used cost minimization to decide which technologies would be the lowest cost for the campus to meet electricity and heating demand. The sensitivity study showed that the results were the most sensitive to energy demand, energy prices, and the carbon tax rate. Although batteries and thermal storage were considered, longer term storage was neglected and it was determined that installation of DER was not cost optimal but could be optimal if a higher carbon tax was established [24].

Yazdanie et al. (2017) optimized the system design using the TIMES (Integrated MARKAL-EFOM System) framework for the DES of Basel in Switzerland for the years of 2010–2050. The technology focus was on boilers, heat pumps, solar thermal, PV, micro combined heat and power (CHP), batteries, and thermal storage. A cost optimization using emission target constraints was performed. Four scenarios were used representing a business as usual scenario, a new energy policy scenario, and a gas variant that allowed for either restricted or unrestricted national imports of natural gas. It was found that building renovations were the most cost optimal measure that could significantly decrease energy demand. In addition, carbon taxes were found to strongly promote low-emission technologies such as heat pumps, rooftop PV, small gas CHPs, and batteries [25].

Lastly, McKenna et al. (2017) created a techno-economic model based on an energy autonomous network in residential buildings for DES. This paper tested various degrees of decentralization with the lowest level being systems within single-family homes to the largest scale of 1000 single family households. The authors developed a MILP model to maximize electrical self-sustainability in the community by selecting the optimal configuration, sizing and operation of micro CHPs, photovoltaics, thermal and electrical storage, and boilers. It was found that cases with larger numbers of prosumers were able to be more electrically self-sufficient and less expensive than single family homes operating as stand-alone systems supplying. Single-family homes operating as stand-alone systems could meet 30% of their electricity needs but districts with more than 560 single family homes met almost 100% of the district's electricity demand. [26]. In this work, the heating demand was not considered in the calculation for self-sustainability and long-term storage options were neglected.

Drawing upon the reviewed publications including future scenarios, the existing studies generally focus on larger energy systems with the smallest being on the scale of a large city [25] and the largest being on the national scale [20]. Many of these large case studies are overly simplified and are not suited to assess the potential of distributed resources and storage, thus it is also important to investigate these scenarios on the decentralized neighbourhood or district level. In addition, many of the publications also lack a comparison of optimal solutions to emissions targets, either on a local or national scale.

1.3. Focus of the study

There is a gap of research in which the future evolution and planning of long-term and short-term storage systems is not yet assessed in a decentralized context. This is summarized by Dodds et al. (2015): *"There is a need to include hydrogen and fuel cell heating technologies in future scenario analyses, and for policymakers to take into account the full value of the potential contribution of hydrogen and fuel cells to low-carbon energy systems"* [27].

Rather than analysing whether implementation of these technologies in DES is feasible today, this study assesses the future predicted potential of storage technologies in DES from 2015 to 2050 using a multi-objective optimization model and then benchmarks the optimal solutions against national carbon dioxide emissions targets for 2020-2050. We investigate the optimal storage configurations using multi-objective optimization to minimize both costs and CO_2 emissions. A particular emphasis is placed on the investigation of long-term hydrogen storage. Today, this technology is quite expensive and is associated with low round-trip efficiencies but is uniquely capable of providing long-term storage while being used in decentralized contexts. In addition, it is predicted to decrease in cost and improve in efficiency over time [5]. The long-term with short-term storage performance is compared for two sample case studies (one rural and one urban) within municipalities in Switzerland including on-site renewable production and local energy demand to demonstrate the ability of the model to evaluate different neighbourhoods. In order to consider the underlying uncertainty of the model inputs from 2015 to 2050, three scenarios and narratives are used that are developed based on the IPCC climate change scenarios [7].

With this goal, the paper is structured as follows. First, the future scenarios are defined and future parameters set in Section 2. Second, the modelling methodology is described in a three-step process that accounts for building energy demands, local renewable potentials, and system modelling in Section 3. Third, the two case studies used for analysis are described in Section 4. Fourth, the results of the optimization are presented and discussed in Section 5. Lastly, conclusions are discussed in Section 6.

2. Future scenario setting

This section introduces the underlying scenarios that are analysed in this study to depict the potential future developments of input parameters and model assumptions. It starts by presenting rationale and background of the scenarios (2.1) and continues with the description of the developed scenarios (2.2), which entails a sketch of the narrative storylines, before the setting of the parameters values for each scenario is outlined (2.3).

2.1. Introduction and development of scenarios

Parameters and assumptions in future energy systems underlie uncertainty regarding their future development, e.g., technology trajectories (learning) and market trends (price volatility). To cope with this uncertainty (i.e., the numerous projections for individual parameters with a broad spectrum of low, medium or high values), scenarios provide a better understanding in order to reach decisions that are robust under a wide range of possible futures [28]. Thus, scenarios are an appropriate tool to assess the alternative images of complex systems by using a consistent set of assumptions within so-called storylines or narratives used to describe the economic, global, and environmental conditions of a scenario [7].

In 2000, the IPCC published the 'Special Report on Emissions Scenarios' (SRES) [7], which contains both quantified projections and narratives (storylines) for the future and which has been extensively used as the reference for subsequent research and for the political and societal discourse on climate change [29]. In the SRES, the IPCC scenarios are based on four narrative storylines that can be categorized along two major dimensions: globalization (from more regional to more global), and sustainability (from more economic to more environmental). These dimensions, along with the resulting storylines, seem to reappear as key archetypical scenarios in a large number of recent international assessments [30]. Fig. 1 shows these scenarios from the original IPCC publication [7].

This study builds upon the IPCC classification and defines three scenarios that are deemed relevant for the investigation of potential future developments from the baseline year 2015 to 2020, 2035, and 2050: (1) Conventional Markets, (2) Global Sustainable Development, and (3) Regional Sustainable Development. These three scenarios,

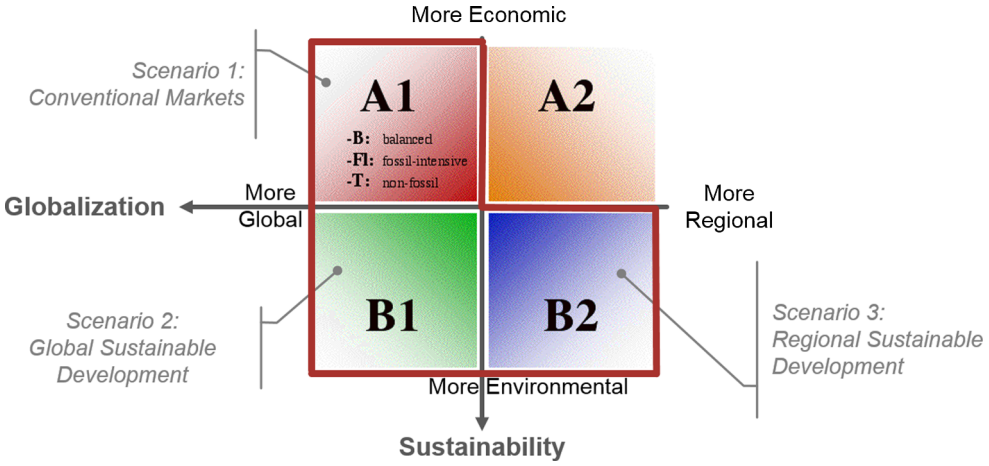

Fig. 1. IPCC Special Report on Emission Scenarios (2000). The red line outlines the three scenarios adapted for this paper [7]. (For interpretation of the references to colour in this figure legend, the reader is referred to the web version of this article.)

shown in Fig. 1, are considered to cover a wide range of possible futures, but certainly not all (e.g., hazardous events, disasters). Thus, they allow using consistent combinations of assumptions composed of the various projections in literature for each parameter (see Section 2.3, Table 1). For this analysis, the A2 scenario was omitted, as in this context it corresponds to transition to more decentralized solutions without a focus on sustainability. This scenario is both unlikely in the Swiss context and would result in neither cheaper nor lower emission solutions in this analysis.

2.2. Description of scenarios

2.2.1. Conventional markets

The *Conventional Markets* scenario (CM) is based on IPCC's scenario A1 and assumes a world of global, well connected markets with a strong economic focus. Since the emphasis rests on fossil-based generation, the deployment of RES remains on a low, business-as-usual level, and consequently the climate is changing more rapidly.

In the Conventional Markets scenario, the energy prices (electricity, gas, oil) are considered to increase only moderately due to high global flow rates and low trade barriers. Because of the economic focus, the feed-in remuneration is phased-out in the short-term, and both the CO_2 tax and the retrofit rate (i.e., pace of efficiency improvements in the building stock) are kept at a rather low, as-is level. As a consequence, technology costs are assumed to be at a high level for RES technologies (e.g., solar PV, wind), at a low level for fossil-based technologies (e.g., oil/gas boiler) and at a medium level for other storage or conversion technologies. For the technology performance, such as efficiencies or lifetime, the relations are inverted. For the building retrofits rate, the current retrofit rate in Switzerland is used, which is defined by the

Table 1
Overview of the three scenarios and selected model-related parameters and assumptions, both on the economic/market and the technology side. (The data below is only an excerpt of the full range of input parameters, which can be found in the appendix.)

			0 Baseline	1 "Conventional Markets"			2 "Global Sustainable Development"			3 "Regional Sustainable Development"		
Parameter		Unit [a]	2015	2020	2035	2050	2020	2035	2050	2020	2035	2050
Economic/Market	Electricity price	CHF/kWh	0.198	0.206	0.235	0.231	0.212	0.251	0.262	0.212	0.251	0.262
	Heating oil price	CHF/kWh	0.067	0.037	0.052	0.061	0.095	0.129	0.148	0.193	0.270	0.305
	Natural gas price	CHF/kWh	0.064	0.094	0.121	0.133	0.109	0.123	0.141	0.096	0.154	0.202
	Feed-in tariff	CHF/kWh	0.176	0.087	0.000	0.000	0.176	0.176	0.176	0.087	0.011	0.001
	Grid CO_2 intensity	g CO_2/kWh	124	150	150	150	100	89	74	0	0	0
	CO_2 tax	CHF/t CO_2	84	84	84	84	120	240	240	120	240	240
	Discount rate	%	6.0	6.0	6.0	6.0	6.0	6.0	6.0	6.0	6.0	6.0
	Retrofit rate	%	1.0	1.0	1.0	1.0	2.0	2.0	2.0	2.0	2.0	2.0
Technology	**Solar PV**											
	Investment cost	CHF/kW	2669	2669	2669	2669	1285	1087	989	1285	1087	989
	O&M cost	CHF/kWh	0.034	0.025	0.019	0.013	0.025	0.019	0.013	0.025	0.019	0.013
	Lifetime	years	25	25	25	25	25	25	25	25	25	25
	Efficiency	%	17.0	17.0	17.0	17.0	17.0	17.0	17.0	17.0	17.0	17.0
	Hydro											
	Investment cost	CHF/kW	3478	3478	3478	3478	3478	3478	3478	3478	3478	3478
	O&M cost	% of inst. kW p.a.	3.0	3.0	3.0	3.0	3.0	3.0	3.0	3.0	3.0	3.0
	Lifetime	years	40	40	40	40	40	40	40	40	40	40
	Wind											
	…	…	…		…			…			…	
	..	..	..		..			..			..	
	.	.	.		.			.			.	

[a] All costs are inflation-adjusted to 2015 CHF (Swiss Francs).

Business as Usual scenario in the Swiss Energy Strategy 2050 to be, on average (actual rates are specific to the age of buildings), 1% of buildings per year [31].

2.2.2. Global sustainable development

The *Global Sustainable Development* (GSD) scenario, resting on IPCC's B1 scenario, pictures a future based on global cooperation, well connected markets but also a strong focus on environmental consciousness and protection. Global regulation puts the fossil phase-out into practice and fosters the deployment of RES, internationally coordinated and mostly in centralized settings, which is why the global temperature increase is more limited than the other scenarios.

In the GSD scenario, the sustainability focus leads to a high tax for emitting CO_2 and a high retrofit rate. The reimbursement for feeding electricity into the grid remains high in the GSD scenario due to a strong grid infrastructure for transmission and distribution for power ex- and imports. Energy prices are expected to increase with a medium rate, as the usage and thus the flow rates for fossil fuels is limited. Since this sustainable scenario relies on the deployment of renewable energy, the cost for RES technologies are assumed to be low, while for fossil-based technologies they remain rather high, and vice versa for their technology performances. In addition, this sustainable scenario includes an increased rate in retrofits defined by the New Energy Policy scenario in the Swiss Energy Strategy 2050 of 2% of buildings, on average, per year [31].

2.2.3. Regional sustainable development

The *Regional Sustainable Development* (RSD) scenario is derived from IPCC's scenario B2 and assumes a shift towards local and decentralized solutions to cope with environmental issues. Similar to the Global Sustainable Development scenario, fossil fuels are phased out, while RES are deployed to a large extent, especially in decentralized settings.

In the RSD scenario, there is also a sustainability focus which leads to a high tax for emitting CO_2 and a high retrofit rate. As opposed to the GSD scenario, in the RSD scenario feed-in rates are slowly phased out as the focus shifts towards self-consumption. Energy prices are expected to increase at a high rate, as the usage and thus the flow rates for fossil fuels is limited, especially in this scenario where additional restrictions (e.g., high import tariffs) hamper both their demand and supply. Since this scenario also relies on the deployment of renewable energy, the technology costs and performances are the same as with the GSD scenario. In addition, the retrofit rate are also be the same as the GSD scenario.

2.3. Setting of future parameters

In order to set the model parameters according to the underlying logic of the above described scenarios, this study relies on projections from literature. If available, projected values were directly sourced from publications, such as the Annual Energy Outlook [32], or are based on ranges (i.e., lower or upper projected limits) given in different sources and referring to the nature (cf. low, medium, high) of each scenarios parameters. Table 1 provides an overview of the three scenarios and selected model-related parameters. Due to the large number of RES, conversion, and storage technologies, the comprehensive set of parameters including references is given in Appendix A.

3. Modelling methodology

The model developed in this work represents a DES with four energy carriers: electricity, heating, gas, and hydrogen. The model optimizes for the configuration and sizing of a selection of storage technologies, conversion technologies, and RES. A schematic representation of the technologies and energy grid included in the model are shown in Fig. 2. Three grids are included in the model: a natural gas grid, a heating grid, and an electricity grid. The RES technologies include small-wind turbines, small-hydro, and solar PV. Conversion technologies include heat pumps, electrolysers, fuel cells, gas turbines, and gas boilers. The storage technologies include battery storage, thermal storage, and hydrogen storage. From the hydrogen storage, a limited portion of hydrogen can be injected directly into the natural gas grid up to a volume concentration of 2%. There is a single set of these conversion and storage technologies that are installed in a centralized location that are connected to the three networks. The output production of these technologies is fed into the networks and is then used to meet the heating and electric demand of the

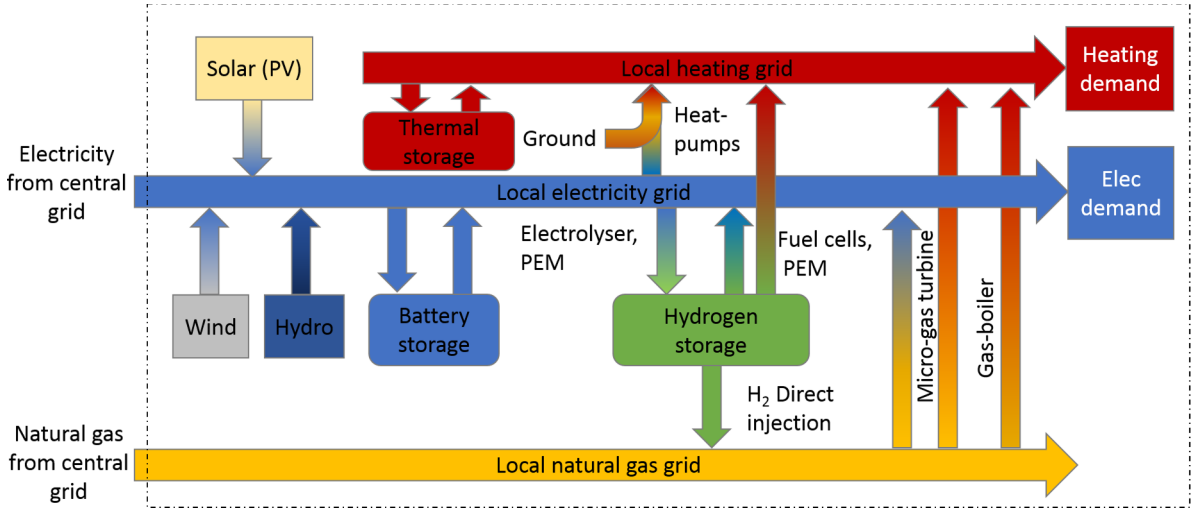

Fig. 2. A Schematic representation of the P2H model with grid interactions.

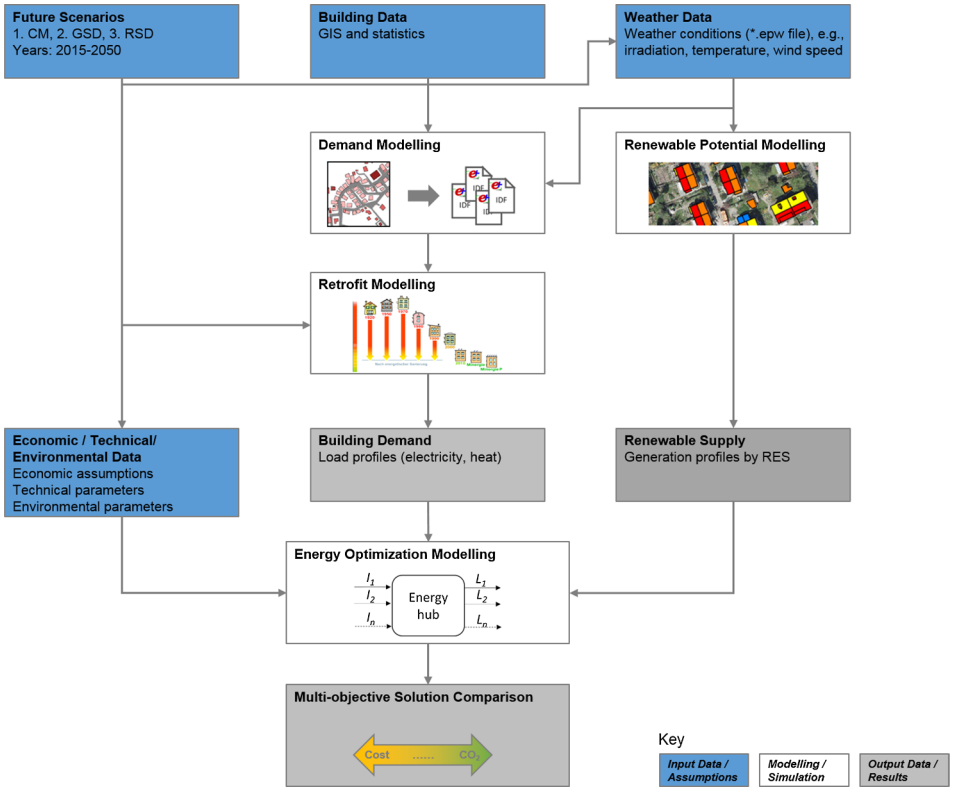

Fig. 3. Modelling work flow and analysis.

neighbourhoods. The costs, efficiencies, and lifetimes of the technologies are found in Tables A.2 and A.3.

The modelling of the DES can be split into three separate categories. First, the buildings demand is simulated for two case studies using a dynamic building model. Second, the renewable energy supply is modelled. Lastly, a multi-objective optimization model that minimizes both costs and CO_2 emissions is run for a full year with an hourly resolution for the baseline year 2015 and the future years 2020, 2035 and 2050 based on the scenarios. According to the objective, the optimal system configuration, sizing, and operation are selected as model outputs. These models are used in the work flow described in Fig. 3.

In this work flow, the process begins through selection of the future scenario and year of consideration. From the selected scenario and year, a weather file is chosen and the building geographic and statistical data are chosen. Based on this weather data (described in Section 4) and the building geography, the demands of the buildings are simulated. In parallel, the renewable potentials pertaining to PV, wind, and hydro are also simulated using weather and geographic data (3.2). The outputs of these two models are the building demands and renewable energy potential profiles for the case studies over a one year period for the present and future years. These profiles are then combined with the set of economic, technical, and environmental parameters (see Table A.1) that are determined based on the year and future scenario and are used as inputs into the optimization modelling (3.3). Finally, the Pareto front for the optimization is shown in Section 5.1 and the Pareto optimal solutions are benchmarked against national energy and emissions building targets described in Section 3.3.6 and shown in Section 5.2.

3.1. Building energy demand

3.1.1. Demand model

In order to calculate the electricity and heating demand in the buildings, the dynamic building model developed in Wang et al. (2018) was used [33]. The CESAR tool utilizes EnergyPlus as a simulation engine to model hourly electricity, space heating, and domestic hot water demand for all buildings considered in the case studies. Using the building 2D geometry available in ArcGIS and the building height, 2.5D building geometry is constructed.

In addition, statistics on building type, building age, and number of occupants is used to estimate both electrical and heating demand at hourly intervals for a year of operation. This data was taken from the Building and Apartment Registry "Gebäude und Wohnungregister") data from the *Bundesamt für Statistik* [34]. It assigns building construction, glazing ratio, and infiltration values based on building age and type. This information is combined into individual EnergyPlus building files for each building, taking neighbouring buildings as shading objects into account. The EnergyPlus files are combined with a weather file and simulated over a one year period at hourly intervals to compute the 2015 base demand for the case studies.

3.1.2. Retrofit modelling

The current retrofit rate for residential buildings lies roughly between 1 and 2% of the building stock. The Swiss Energy Strategy 2050 has outlined retrofit rates based on building type (single or multi-family houses) and building age for the 'Weiter wie Bisher' scenario (equivalent to 'business as usual') and the 'Neue Energiepolitik' scenario (equivalent to 'new energy policy') [31]. Based on these retrofit rates, buildings within the case studies are selected to be retrofitted and their constructions are updated. The future demand is then calculated for the years of 2020, 2035, and 2050 using updated EnergyPlus files.

3.2. Renewable potential modelling

For both case studies, the renewable potentials within the DES boundaries are examined. As the case studies include both rural and urban settings, geographical information system (GIS) data was used to

assess the amount of land on the building parcels and the natural resources in the immediate area. Light detection and ranging (LiDaR) data for both terrain and building elevation were acquired from Swisstopo (2014) [35] for both case studies to evaluate the rooftop geometry for available solar installations, as well as the shading from the terrain in the area. As decentralized renewables were the focus, wind or PV farms were not included, but rather rooftop PV and small-wind potential that is suitable for installation in more populated areas.

3.2.1. Rooftop photovoltaics

A GIS approach based on the method developed in Mavromatidis et al. (2015) [36] is used to derive the hourly solar radiation on the rooftops, as well as to calculate the available area for solar installations. Using LiDaR data for the building elevation and digital terrain raster data from Swisstopo, the rooftop slopes, aspects, area, and solar incidence on rooftop surfaces are calculated at a 2 m × 2 m resolution in ArcGIS for all non-protected buildings in the two case studies. The efficiency of the PV panels is then calculated at each time interval using efficiency correlations based on the temperature of the panels. For more details, please refer to Mavromatidis et al. [36].

3.2.2. Small-wind

Due to the low average wind speeds in the case studies, a low speed wind turbine is proposed. The selected model was the Aventa LoWind Turbine [37]. At a hub height of 18 m, the corrected wind speed was calculated with Eqs. (1) and (2).

$$u = u_r \left(\frac{z}{z_r} \right)^{\alpha} \tag{1}$$

$$\alpha = \frac{ln(u_2) - ln(u_1)}{ln(z_2) - ln(z_1)} \tag{2}$$

Here, u represents the corrected wind speed, u_r represents the reference wind speed at a certain height, z is the height of the wind turbine, z_r is the height at which the reference wind speed is taken, and α is a coefficient that represents the rate of wind speed increase as a function of height that can be solved with Eq. (2). The power curve for the selected wind turbine was then used to correlate hourly power production depending on the corrected wind speed.

3.2.3. Small-hydro

The potential of a micro hydro plant is assessed for a river in one of the case studies. Flow rates are provided for a potential site in the nearby river that is currently not utilized for hydropower. These measured volumetric flow rates are aggregated into hourly intervals to calculate the available energy potential over the year using Eq. (3),

$$P = \eta \rho g Q H \tag{3}$$

In Eq. (3), P is the generated hydropower in kWh, η is the turbine efficiency, g is the acceleration due to gravity, Q is the volumetric flow rate in m^3/s, and H is the effective pressure head of water across the turbine in meters. In this case, the turbine efficiency is assumed to be 80%, as it is a smaller turbine in a micro-hydro plant [38].

3.3. Energy optimization modelling

For the DES model, multi-objective optimization with mixed-integer linear programming (MILP) was applied. This type of modelling is based on the energy hub concept [8]. In this model, multiple energy carriers (electricity, heat, hydrogen, and natural gas) are balanced from primary energy input to end energy demand according to a series of constraints that represent conversion technologies, storage technologies, distribution grids, and other factors. In this type of optimization, the decision variables represent the selection of the technology configuration, technology sizes, and operation of the technologies for hourly time steps over a one year period (8760 h). The model optimizes the sizes of the technology units, unit performance, network performance, and operation of the system.

Rather than using the typical days or rolling horizon methods for this optimization, a full horizon (8760 hourly time steps) is used to accurately assess the long-term storage system potential in the model. The model was programmed using the Python API for IBM ILOG CPLEX Optimization Studio and was solved using a CPLEX solver on a cluster computing machine.

3.3.1. Dispatchable conversion technologies

Dispatchable conversion technologies include heat pumps (HP), gas boilers (GB), micro-gas turbines (MGT), polymer electrolyte membrane fuel cells (PEMFC), and polymer electrolyte membrane electrolysers (PEMEC). The operation parameters of each technology are based on the sizing of the technology in kW. All dispatchable conversion technologies contain maximum and minimum capacity constraints that are described in Eqs. (4) and (5).

$$P^c_{t,out} \leqslant Cap^c \ \forall \ t = 1, ..,8760, \ \ C \tag{4}$$

$$P^c_{t,out} \geqslant Cap^c * PLR^c_{min} \ \forall \ t = 1, ..,8760, \ C \tag{5}$$

Here, $P^c_{t,out}$ is the power output for each of the dispatchable conversion technologies in set C, Cap^c is the maximum power of the conversion technology (PEMEC, PEMFC, MGT, GB, and HP) which is determined by its sizing, and PLR^c_{min} is the minimum part load of the technology.

3.3.1.1. Electrolysers. Electrolysers are the first component in the P2H storage configuration. Although technically a conversion technology, electrolysers consume electricity and produce hydrogen that can be stored. Polymer electrolyte membrane electrolysers (PEMEC) were chosen for this model due to their quick responsiveness, flexibility, ability to withstand higher degrees of cycling than alkaline electrolysers, and ability to produce pressurized H_2 [4]. In this paper, the PEMEC is assumed to produce hydrogen at a pressure of 10 bar. The model for PEMECs was not developed in this work but in a joint project that aimed to produce reduced order models for electrolysers and fuel cells for optimization. The model for PEMECs is found in Gabrielli et al. (2018) [39] and uses a piecewise affine (PWA) linear relationship based on four linear segments to represent the part-load efficiency curve or the produced hydrogen in Nm^2/kWh. The PWA assumption is modelled using one binary segment for each section, and only one of these binaries can be one at any given time step.

3.3.1.2. Fuel cells. Fuel cells are the second technology included in the P2H configuration. They are considered a CHP technology that runs on hydrogen. Unlike most CHP technologies, PEMFCs have a higher electrical efficiency than a thermal efficiency. PEMFCs were chosen due to their increased flexibility and responsiveness as opposed to solid-oxide fuel cells [4]. Solid-oxide fuel cells have higher electric efficiencies, however their high temperature operation (700–1000 °C) results in a slow response to changes in load. Due to the complex performance curve of PEMFCs, PWA linear relationship also from Gabrielli et al. (2018) [39] was used to simulate the part-load electrical efficiency curve. To estimate the heat production, the total efficiency of the fuel cell was fixed at 95%, and the difference between total and electrical was approximated as the heat production efficiency. Although not directly a storage technology, in this model the running of the PEMFC indicates discharging of the hydrogen storage to produce electricity and heat.

3.3.1.3. Micro-gas turbines. Micro-gas turbines are micro CHP devices that run on natural gas. They are modelled based on Capstone MGT which provides their efficiency curves for both electricity and heat for all of their MGT sizes on their website [40]. A linear approximation of this curve is then used for both electricity and heat.

3.3.1.4. Gas boilers. Gas boilers were modelled using a linear efficiency curve with a nominal efficiency of 90% and a minimum part-load restriction of 5%.

3.3.1.5. Heat pumps. Ground-source heat pumps were considered over air source heat pumps due to the low temperatures of the case studies in winter. A linear correlation between COP and the heat source temperature from Sanner (2005) [41] was used to model the heat pumps. This relationship is dependent on the heat source temperature and the delivered heat temperature which was assumed to be 70 °C. The number of heat pumps installed in each case study is limited by the number of boreholes available for placement. A GIS analysis for each case study was performed on the parcel area that the buildings are situated on. Boreholes are then placed with a minimum radius of 10 m apart from each other and from buildings. For more details on the GIS borehole placement, please refer to Miglani et al. (2016) [42].

3.3.2. Non-dispatchable renewables

Photovoltaic panels, small-wind turbines, and small-hydro are non-dispatchable technologies. The modelling of the PV, small-wind turbines, and small-hydro have been described in Section 3.2. This modelling represents the yearly maximum output potential profile calculated and is imported into the model. PV and wind sizing is performed using integer decision variables with 1 PV unit representing 1 m^2 of panel area and one wind unit representing one 6.5 kW turbine. As the size of the 2.3 MW small-hydro station is fixed, it is modelled with a single binary decision variable. The actual output produced in each hour from each non-dispatchable technology is scaled for each technology relative to the fraction of actual installed potential over the maximum potential.

3.3.3. Storage technologies

Three storage systems are modelled in this work: hydrogen storage, batteries, and thermal storage. Although both long-term and short-term storage systems are considered in this work, it should be noted that the exact length of the charge and discharge cycle for each storage technology is selected by the optimizer and that long-term and short-term storage systems are not considered separately or are modelled differently. Any three of the storage systems can be chosen for either long-term or short-term storage. Hydrogen storage tends to be optimal for long-term storage as it does not have time dependent losses. In contrast, batteries and thermal storage both have significant time dependent losses (0.1 and 1% of stored energy hourly respectively) resulting in a significant decay of energy when used over longer time horizons. Over short time horizons, batteries and thermal storage tend to be optimal as they have higher round-trip efficiencies (for the electric and heating energy carriers respectfully), although hydrogen storage can occasionally be used over short-time horizons.

3.3.3.1. Hydrogen storage. The hydrogen produced from the electrolyser is stored in compressed gaseous cylinders up to 90 bars of pressure. The compression energy is calculated with Eqs. (6) and (7).

$$W_{ideal} = \overline{Z} R T_1 \frac{\gamma}{\gamma - 1}\left[\left(\frac{P_2}{P_1}\right)^{\frac{\gamma-1}{\gamma}} - 1\right] \tag{6}$$

$$P_{comp} = \dot{n}\frac{W_{ideal}}{\eta_{isentropic} * \eta_{motor}} \tag{7}$$

In Eq. (6), $\overline{Z}$ is the compressibility factor of hydrogen at a certain temperature and pressure, R is the ideal gas constant in kJ/kmol K, T_1 is the inlet temperature in Kelvin, P_1 and P_2 are the inlet and outlet pressures respectfully, and γ is the specific heat ratio of the gas (C_p/C_v). This computes the work of isentropic compression as a function of the final pressure per unit mass. The electricity of compression is calculated with Eq. (7), where $\dot{n}$ is the molar flow rate of hydrogen production, $\eta_{isentropic}$ is the isentropic efficiency of the compressor, which is assumed to be 80% [10] and η_{motor} is the mechanical efficiency of the electric motor, which is assumed to be 90%. The sizing of hydrogen compressors is performed based on required electricity to compress the maximum hourly hydrogen production flow rate in the year. The state of charge of the hydrogen tank is calculated at each hourly time step with Eq. (8).

$$M_t^{H2} = M_{t-1}^{H2} + \dot{m_{PEMEC}}\Delta T - \dot{m_{PEMFC_{fuel}}}\Delta T - \dot{m_{DI}}\Delta T \tag{8}$$

$$M_t^{H2} \leqslant Cap^{H2} \tag{9}$$

In this equation, it is assumed that the decay of the storage in the tank is zero (i.e., has no leaks) and that the system has an efficiency of 99% on discharge. In addition, direct injection of natural gas into the grid is assumed to not require additional compression power as it is being injected into the low pressure part of the gas grid which is typically less than 70 bars in European gas grids compared to the 90 bar stored in the hydrogen tanks. The hydrogen storage maximum capacity is sized in *kg* of hydrogen. In addition, the seasonal storage component of the simulation must be included to initialize the first time step of the year to be of the same state of charge of the last time step, as is shown in Eq. (10).

$$M_{t=1}^{H2} = M_{t=8760}^{H2} \tag{10}$$

3.3.3.2. Batteries and thermal storage. Simplified battery and thermal storage models are assumed for this work. The models are described in Eqs. (11)–(13), with Eq. (11) describing the energy balance in both storages, Eq. (12) restricting the state of charge below the capacity, and Eq. (13) limiting the maximum discharge and charge rates.

$$E_t^s = E_{t-1}^s \cdot Decay^s + \eta_{Charge}^s \dot{P}_{Charge}^s \Delta T - \frac{1}{\eta_{Discharge}^s}\dot{P}_{Discharge}^s \Delta T \quad \forall \quad S \tag{11}$$

$$E_t^s \leqslant Cap^s \quad \forall \quad S \tag{12}$$

$$P_{Charge/Discharge}^s \leqslant Cap^s \delta_{Charge/Discharge}^s \quad \forall \quad S \tag{13}$$

Here, S is the set of non-hydrogen storage technologies (batteries and thermal storage) E_t^s is the storage level in the battery or thermal storage, $P_{Charge/Discharge}$ are the charge and discharge powers in kW, $\eta_{Charge/Discharge}$ represents the charging and discharging efficiencies, and $Decay^s$ is the rate at which the stored energy decays in an hour. For this model, the efficiency of lithium-ion batteries were assumed, thus the charging and discharging efficiencies are both equal to 92% and the decay is set to 0.1% per hour. For the thermal storage, the charging efficiency, discharging efficiency, and decay are set based on the work of Stadler et al. (2008) [43] to 90%, 100%, and 1% per hour. $\delta_{Charge/Discharge}$ describes the limit on the discharge and charging rates as percent of maximum capacity that can be charged or discharged within an hour. For batteries, based on a C-rate of 0.5C, this is assumed to be to 50%. For thermal storage, this is set again by Stadler et al. to be 25% [43]. Similar to the hydrogen storage, there is also a constraint ensuring that the stored energy level at the beginning and end of the year are equal to each other. This is shown in Eq. (14).

$$E_{t=1}^s = E_{t=8760}^s \quad \forall \quad S \tag{14}$$

3.3.4. Energy grid modelling

In the model, network grids for electricity, heating, and natural gas were included. A transformer efficiency to the low-voltage grid of 98% was assumed. The heating network is approximated with a minimum spanning tree network from the energy centre in the middle of the neighbourhood to the building centroids. A heating loss rate of 4.3% per km of heating pipe is assumed [44]. Electric pumping power is taken to be 8.5% of the total heating demand in each time step [45].

Direct injection of hydrogen into the natural gas grid is also allowed

for up to a 2% limitation by volume (the recommended value for networks with turbines [46]). This condition is enforced by Eq. (15).

$$V_t^{DI,H2} \leqslant (V_{in,t}^{MGT,NG} + V_{in,t}^{GB}) \cdot 0.02 \quad \forall \ t \tag{15}$$

Here, $V_t^{DI,H2}$ is the amount of hydrogen injected into the natural gas grid, $V_{in,t}^{MGT,NG}$ is the natural gas consumed by the MGT, and $P_{in,t}^{GB}$ is the natural gas consumed by the boiler.

The energy content of both gases can be converted using their heating values, which are approximately 39.4 and 14.5 kWh/kg for hydrogen and natural gas respectively.

In the model, the three grids are assumed and are simultaneously balanced with constraints to ensure that supply meets demand. The balance for electricity, heating, and natural gas in the network are shown in Eqs. (16)–(18) respectively.

$$\begin{aligned} &\frac{P_{grid,t}^{Pur}}{\eta_{trans}} + P_{out,t}^{PV} + P_{out,t}^{Wind} + P_{out,t}^{Hydro} + P_{out,t}^{MGT} + P_{out,t}^{FC} + Pdischarge_{t,s}^{Battery} \\ &\quad = Demand_t^{elec} + Pcharge_t^{Battery} + P_{in,t}^{HP} + P_{in,t}^{EC} + P_{in,t}^{Comp} + P_{aux,t}^{pump} + P_{grid,t}^{sell} \\ &\quad + P_{grid,t}^{sellFIT} \ \forall \ t \end{aligned} \tag{16}$$

$$P_t^{GB} + P_t^{FC} + P_t^{MGT} + P_t^{HP} + Pdischarge_{t,s}^{TES} = \frac{Demand_t^{Heat}}{\eta^{losses}} + P_t^{dump} + Pcharge_t^{TES} \ \forall \ t \tag{17}$$

$$P_{grid,t}^{NG} + P_t^{DI,H2} = P_{in,t}^{MGT} + P_{in,t}^{GB} \ \forall \ t \tag{18}$$

Since the model can install several technologies at once, multiple devices can be simultaneously run to provide either electricity or heating demand in any given time step. There is no set utilization priority, but rather the technology utilization is an outcome of the model that decides during each time step which devices are the most optimal in order to meet the energy demands based on the respective objective function of the optimization.

3.3.5. Multi-objective optimization

Multi-objective optimization is used to minimize both system costs and carbon emissions. The system costs are calculated using Eqs. (19)–(25).

$$Cost_{total} = Cost_{inv} + Cost_{OMF} + Cost_{OMV} + Cost_{elec} + Cost_{fuel} \tag{19}$$

Here, $Cost_{total}$ is the cost objective to be minimized, $Cost_{inv}$ is the equivalent annual investment cost of the technologies, $Cost_{OMF}$ is the fixed operation and maintenance costs, $Cost_{OMV}$ is the variable operations and maintenance costs, $Cost_{elec}$ is the electricity cost, and $Cost_{fuel}$ represents the fuel costs. The investment costs are calculated with Eq. (20).

$$Cost_{inv} = \sum_{c=1}^{C} (Cost_c \cdot Cap_c \cdot CRF_c) + \sum_{s=1}^{S} (Cost_s \cdot Cap_s \cdot CRF_s) \tag{20}$$

In Eq. (20), C represents the set of conversion and S represents the set of storage technologies, *Cost* represents the capital cost of the technologies per unit of capacity installed, and *Cap* is the capacity of each technology installed in kW. Capital recovery factor (*CRF*), or equivalent annual cost factor is calculated for each technology based on its rated lifetime in years. To calculate the CRF factor, Eq. (21) is used [47].

$$CRF_{c,s} = \frac{r}{\left[1 - \frac{1}{(1+r)^{Lifetime_{c,s}}}\right]} \ \forall \ c, s \tag{21}$$

Here, r is the discount rate, and *Lifetime* is the expected age of the technology in years. The operations and maintenance costs are then calculated with Eqs. (22) and (23).

$$Cost_{OMF} = \sum_{c=1}^{C} (OMF_c \cdot Cap_c) + \sum_{s=1}^{S} (OMF_s \cdot Cap_s) \tag{22}$$

$$Cost_{OMV} = \sum_{c=1}^{C} \left(OMV_c \cdot \sum_{t=1}^{8760} P_{c,t}^{out} \right) + \sum_{s=1}^{S} \left(OMV_s \cdot \sum_{t=1}^{8760} Discharge_{s,t} \right) \tag{23}$$

Fixed operations costs (*OMF*) are calculated based on the technology sizes (*Cap*) and variable operations costs (*OMV*) are calculated based on the operational output of the technologies over the one year period. For conversion technologies, this is defined by the output energy in kWh over the year ($P_{c,t}^{out}$). For storage technologies, this is defined by the discharge energy in kWh over the one year period ($Discharge_{s,t}$). The last two costs are fuel and electricity costs, as shown in Eqs. (24) and (25).

$$Cost_{fuel} = \sum_{t=1}^{8760} (P_{grid,t}^{NG} \cdot Price^{NG}) \tag{24}$$

$$Cost_{elec} = \sum_{t=1}^{8760} (P_{grid,t}^{Pur} \cdot Price_t^{Retail}) - \sum_{t=1}^{8760} (P_{grid,t}^{Sell} \cdot Price_t^{MP}) - \sum_{t=1}^{8760} (P_{grid,t}^{SellR} \cdot Price_t^{FIT}) \tag{25}$$

In Eq. (24), $P_{grid,t}^{NG}$ represents the natural gas purchased from the grid in each time step and $Price_{grid,t}^{NG}$ is the fuel price.

Electricity cost represents the cost and profit from interactions of the decentralized network with the central electricity grid. Electricity from the grid ($P_{grid,t}^{Pur}$) is purchased at the retail price of electricity in CHF/kWh. Retail price represents the price of electricity that is purchased from an electric utility. This price is typically constant or uses a two-tiered high and low tariff pricing scheme for peak hours and off-peak hours of use in Switzerland. In this case, a constant rate is used. Electricity sold back to the grid is split into two categories for renewable electricity and for non-renewable electricity. Electricity sold from RES technologies ($P_{grid,t}^{SellR}$) like PV, hydro, and wind, can be sold at the feed-in tariff rate. The feed-in tariff is an incentive for renewable production such as PV, small-hydro, and wind. Electricity sold from all other devices ($P_{grid,t}^{Sell}$) is sold back at the market price (MP) of electricity. The market price represents the real price of electricity for either buying or selling (in this case selling), which fluctuates due to supply and demand on the national grid level. Its prices are typically two to three times lower than the retail price. Although battery storage or fuel cell output can indirectly come from renewable energy, in this model the electricity discharged from storage devices cannot be sold to the grid at the feed-in tariff rate. To incentive local use of renewable energy, there is a constraint to ensure that only surplus electricity from renewable devices during each time step can be sold back at the feed-in tariff price. This constraint is shown in Eq. (26).

$$P_t^{SellR} \leqslant (P_{out,\ t}^{PV} + P_{out,\ t}^{Hydro} + P_{out,\ t}^{Wind} - Demand_t^{elec}) \cdot \delta_t^{surplus} \ \forall \ t = 1, ..,8760 \tag{26}$$

Here, $\delta_t^{surplus}$ is a binary variable that is 1 if $P_{out,\ t}^{PV} + P_{out,\ t}^{Hydro} + P_{out,\ t}^{Wind} > Demand_t^{elec}$ (i.e., a surplus) and 0 if $P_{out,\ t}^{PV} + P_{out,\ t}^{Hydro} + P_{out,\ t}^{Wind} \leqslant Demand_t^{elec}$ (i.e., a deficit). This constraint ensures that electricity can only be sold back at the feed-in tariff rate if the production of renewables is greater than the electricity demand. In addition, the amount of energy that can be sold at the feed-in tariff rate is limited by the difference between the renewable production (hydro, PV, and wind) and the electric demand.

The annual CO_2 emissions, in kg CO_2/kWh are calculated with Eq. (27).

$$CO2_{total} = \sum_{t=1}^{8760} (P_{grid,t}^{NG} \cdot CF^{NG} + P_{grid,t}^{Pur} \cdot CF^{elec}) \tag{27}$$

Here, *CF* is the carbon factor in kg CO_2/kWh for natural gas and the electricity intensity in the grid.

With both the objective functions defined, multi-objective optimization is then performed with the epsilon-constraint method [48]. In this method, the optimization is first solved with only a cost objective

and the CO_2 emissions are calculated consequently. Secondly, the problem is solved with a CO_2 minimization objective. To solve for multi-objective cases, the epsilon value is calculated at even intervals between the maximum (cost optimal) and minimum (CO_2 optimal) emissions, and then the total emissions are constrained below these epsilon values while optimizing for minimum costs, resulting in multiple intermediate optimal solutions. In this study, five Pareto optimal solutions are chosen to give a variety of solutions for each set of parameters. For the purpose of this study, the 5 Pareto optimal solutions will be referred to as the *cost minimization*, *25% CO_2 objective minimizationb*, *50% CO_2 objective minimization*, *75% CO_2 objective minimization*, and *CO_2 minimization* solutions. The percent referred to is not a reduction of the total emissions but rather the percent reduced relative to the difference between the cost minimization and CO_2 emission minimization objectives.

In order to compare the results across the two case studies on a fair basis, the *Levelized Cost of Energy (LCOE)* and *Levelized CO_2 Emissions* (LCO2) for DES will be used. The $LCOE_{DES}$ is defined as the total annual costs of the energy system (defined in Eq. (19)) divided by the sum of the total annual electricity and heating demand. The $LCO2_{DES}$ is defined as the total annual emissions (defined in Eq. (27)) divided by the sum of the total annual electricity and heating demand. The calculation of $LCOE_{DES}$ and $LCO2_{DES}$ are shown in Eqs. (28) and (29) respectively. These terms will be used in Section 5.

$$LCOE_{DES} = \frac{Cost_{total}}{\sum_{t=1}^{8760} (Demand_t^{elec} + Demand_t^{heat})} \tag{28}$$

$$LCO2_{DES} = \frac{CO2_{total}}{\sum_{t=1}^{8760} (Demand_t^{elec} + Demand_t^{heat})} \tag{29}$$

The terms $Demand_t^{elec}$ and $Demand_t^{heat}$ in Eqs. (28) and (29) refer to the hourly demand of all buildings simulated in Section 3.1.

3.3.6. Energy strategy targets

In order to benchmark solutions against the targets of the Swiss Energy Strategy, the Kaya Identity is used. The emissions targets are not included in the optimization but used in Section 5 to benchmark the solutions for the years of 2020, 2035, and 2050. The calculation of these energy targets for buildings is defined in Mavromatidis et al. (2016) [49] in reference with the Swiss Energy Strategy 2050 [31]. This paper uses the Kaya identity to calculate the emissions targets based on Eq. (30).

$$C = \frac{C}{E}\frac{E}{A}A \tag{30}$$

Here, C refers to the total Swiss CO_2 emissions targets from buildings (in this case in $kgCO_2$), E refers to the total energy consumption in buildings (in kWh), and A refers to the total floor area in buildings (in m^2) at 2020, 2035, and 2050 defined in the strategy. Both the floor area for all buildings and the CO_2 targets are defined in the strategy at the years of 2020, 2035, and 2050. As the total emissions for all buildings and the floor area of all buildings are fixed in the energy strategy at each year, the $\frac{C}{E}$ and $\frac{E}{A}$ can both be adjusted to meet the targets. The term $\frac{C}{E}$ refers to the CO_2 intensity per kWh of energy produced in buildings. The value of $\frac{C}{E}$ decreases with an increasing percentage of RES being used to meet energy demand and increases when the percentage using fossil fuels increases. The term $\frac{E}{A}$ refers to the energy density of buildings per unit area, which represents the energy efficiency of the building envelope. The more inefficient the buildings are (i.e., older building stock), the higher the energy density is. When buildings are retrofitted, their kWh/m^2 decreases, thus this value decreases from 2015 to 2050 based on increasing number of retrofitted buildings. The model optimization chooses the level of renewables on the system side, thus optimizing the $\frac{C}{E}$. The resulting optimization solutions can be compared against the official targets according to the energy strategy, which are shown in dashed lines in Figs. 7 and 8.

4. Case study descriptions

There are two case studies used in this paper representing a rural and urban neighbourhood respectfully. These two types of neighbourhoods represent two typical examples of neighbourhoods within Switzerland. The comparison of these two highlights the differences in system design depending on RES and energy density in design locations. The total area of heated and electrified space in the buildings is defined in the building energy demand models (3.1) and this can be used to compare the energy density in the buildings (in kWh/m^2) and the LCO2, which are key performance indicators in relation to the Swiss Energy Strategy 2050 and its targets for decarbonization in the Swiss building stock. This allows the two case studies to be benchmarked against each other and to the Swiss emission targets.

4.1. Zernez

Zernez is a rural alpine village in the Swiss Alps with approximately 1150 people inhabiting 308 buildings. The building stock consists of mostly of single-family homes, multi-family homes, shops, hotels, restaurants, and agricultural buildings. It is located at an altitude of 1475 m resulting in a cold climate with an average temperature of 4.7 °C. A small river that passes by the village is planned for a small 2.3 MW run-of-the-river small hydro plant. It is approximated from a GIS analysis that 60 small-wind turbines at a hub high of 18 meters could be placed in the vicinity of the village. In addition, there is 25,200 m^2 of rooftop area available for PV installation excluding protected buildings. More data on this case study can be found in [50].

4.2. Altstetten

Altstetten is a populated and primarily residential quarter in the city of Zurich in Switzerland. A section of 77 buildings in Altstetten was chosen as it was scaled to nearly the same total annual demand as Zernez. These buildings consist of primarily multi-family homes and shops with a population of 1784 inhabitants. Statistics on the buildings is available from the Swiss Buildings and Apartments Registry (GWR) [34]. As a result, it has a higher population density than Zernez. As it lies in a city, small wind and hydro are not available as renewable resources and 12,080 m^2 is available for rooftop PV area.

The incident radiation of the rooftops calculated in the two case studies is shown in Fig. 4.

4.3. Future demand data for case studies

In order to predict future demand for buildings, two factors are considered: retrofits and climatic weather changes. Based on the 2015 baseline year, the demand model (3.1.1) was used to calculate individual demand for all buildings in Zernez and Altstetten. The baseline year is simulated with a typical meteorological weather file from both locations specifically. Future demand for the years of 2020, 2035, and 2050 are calculated with the retrofitting model (3.1.2). Using this model, retrofits are applied and building constructions are updated at future years of consideration. In addition, weather files considering climate change in the future were obtained from Meteonorm based on the work published in Remund et al. (2010) [51]. The weather files in this work are based on the IPCC A1B and B1 scenarios. For the future demand, the CM scenario was chosen to use the Business as Usual scenario retrofit rates and the A1B weather files, the GSD scenario was chosen to use the New Energy Policy scenario retrofit rates and the B1 weather files, and the RSD scenario was chosen to use the New Energy Policy retrofit rates and the A1B weather files. Since the B2 weather files are not yet available for these locations, the A1B is used in its place

Fig. 4. Solar radiation potentials of the cases with Zernez on the left and Altstetten on the right.

as the warming predicted in the B2 scenario on average globally falls in the range predicted by the A1B scenario. A summary table of the temperatures in the weather file are shown in Table 2. The results of the aggregated demand for these case studies are shown in Fig. 5. In this Figure, three scenarios (which are Conventional Markets, Global Sustainable Development, and Regional Sustainable Development) are shown from 2015 to 2050. The heating demand decreases over time due to more buildings being retrofitted each year in both neighbourhoods. When these buildings are retrofitted, windows, facade, floor, and roof insulation are all added to reduce the heating demand. In addition, the electrical appliances and lighting are updated to increase their efficiency and decrease the electrical energy demand in the buildings. The GSD and RSD scenarios have an average retrofit rate 2% of buildings per year compared to the CM rate of 1%, thus they are able to retrofit twice the number of buildings, resulting in a lower demand. In addition, the buildings are simulated with the relevant weather files, with the A1B (used by CM and RSD scenarios) scenario having higher warming than the B1 (GSD) scenario. As a result, the RSD has a lower heating demand over time compared to the GSD scenario despite having the same retrofit rate, as the RSD has a warmer average temperature and thus less heating demand than the GSD scenario.

4.4. Future renewable potential vs. demand

In addition to the electricity and heating demand for the buildings, the renewable potentials are also calculated in the model. As the change in wind speeds and solar potential are not considered and updated in future weather files, these renewable potentials are assumed to remain the same over time. It is predicted that the demand decreases due to retrofits as the renewable potential remains constant. This is represented in Fig. 6. In this Figure, the surplus or deficit is calculated by subtracting the total energy demand in each hour from the total renewable production in each hour and then summing up the monthly totals. It can be observed that the surplus for both case studies grows over time due to the lower demand in 2050 compared to 2015. In addition, Zernez has a much higher amount of renewables, resulting in a greater surplus.

In Fig. 6, the level of surplus renewables (i.e., times of higher renewable potential than demand) increases over time, especially in the Zernez case. With extra surplus energy, the optimization may decide to install less renewables, to install the renewables but sell production to the grid, or to use storage technology to shift the energy surplus to later energy deficit.

Table 2
Weather file average temperature for the future scenarios, years, and locations.

Region	Parameter	2015	2020		2035		2050	
		Baseline	A1B	B1	A1B	B1	A1B	B1
Global	Mean temp vs. 1980–1999 (Δ °C)	+0.4	+0.7	+0.5	+1.2	+1.0	+1.7	+1.3
Zernez	Max temp (°C)	25.1	24.3	24.7	27.6	26.3	27.7	26.3
	Mean temp (°C)	4.4	4.9	4.9	5.5	5.2	6.1	5.5
	Min temp (°C)	−20.0	−16.3	−15.9	−15.9	−16.6	−16.0	−16.1
Altstetten	Max temp (°C)	29.9	32.3	33.0	33.0	33.8	32.9	33.3
	Mean temp (°C)	8.7	10.4	10.4	11.0	10.7	11.5	11.0
	Min temp (°C)	−10.4	−8.6	−8.2	−8.1	−9.0	−7.6	−8.1

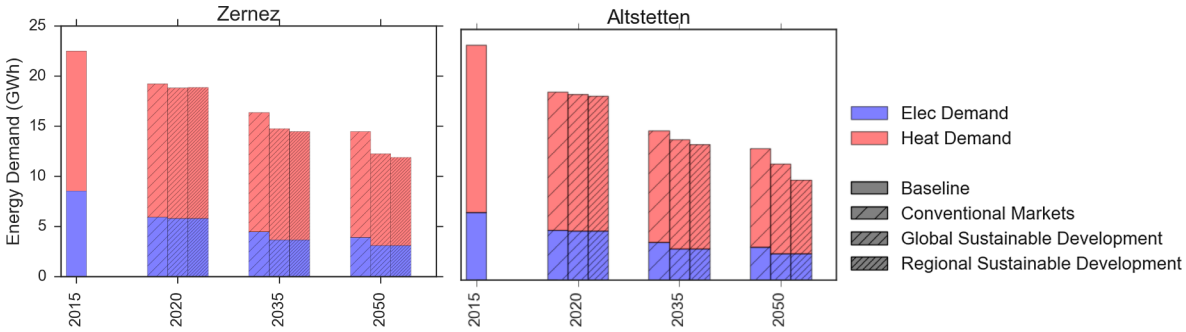

Fig. 5. Future building energy demand of Zernez (left) and Altstetten (right).

5. Results and discussion

Based on the scenarios formulated in Section 2, a series of simulations were conducted to evaluate the scenarios using the multi-objective method to find a set of Pareto optimal solutions.

5.1. Pareto fronts

Fig. 7 shows the Pareto fronts for all of scenarios, years, and objectives simulated with the $LCOE_{DES}$ on the x-axis and LCO2 on the y-axis. In multi-objective optimization, the solutions show the set of Pareto optimal solutions according to the two objectives. The energy strategy targets are included in dashed lines. Please note that the targets differ from the CM scenario to the GSD and RSD scenario due to the difference in the assumed CO_2 intensity of the electricity grid (please see Table A.1 for details). The Pareto curves, moving from upper-left and cost optimal to lower-right and CO_2 optimal, show five different solutions that are all on the spectrum from fully cost optimal to fully CO_2 optimal. From 2015 to 2050, the subsequent years' emissions drop lower, indicating that more renewable sources are being used to meet a higher fraction of the demand over time. In addition, many of these solutions are also dropping in cost over time as the capital costs of technologies decrease. For the Zernez case study, much larger emission reductions can be achieved due to the higher renewable potential. Emission reduction in the Altstetten case study is more restricted due to the lower renewable potential available.

For both case studies, the Pareto curves initially have a steep drop in emissions followed by shallow and rapid increase in costs. This indicates that a large portion emissions reduction can be met without a high increase in the costs, however the costs rapidly increase above the 75% CO_2 minimization solution. A full breakdown of costs by type is shown in Fig. B.1 in the Appendix B. As seen in this Figure, the rapid

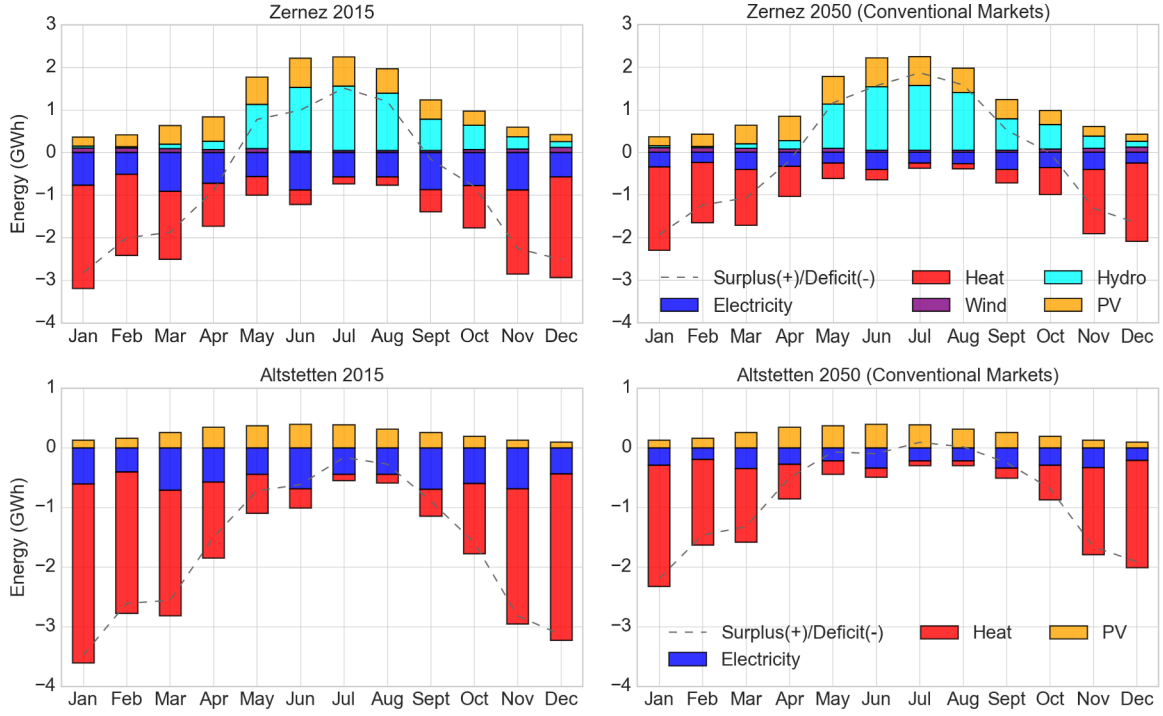

Fig. 6. Renewable potential (positive) and demand (negative) for Zernez and Altstetten in the 2015 Baseline year and the CM scenario in 2050.

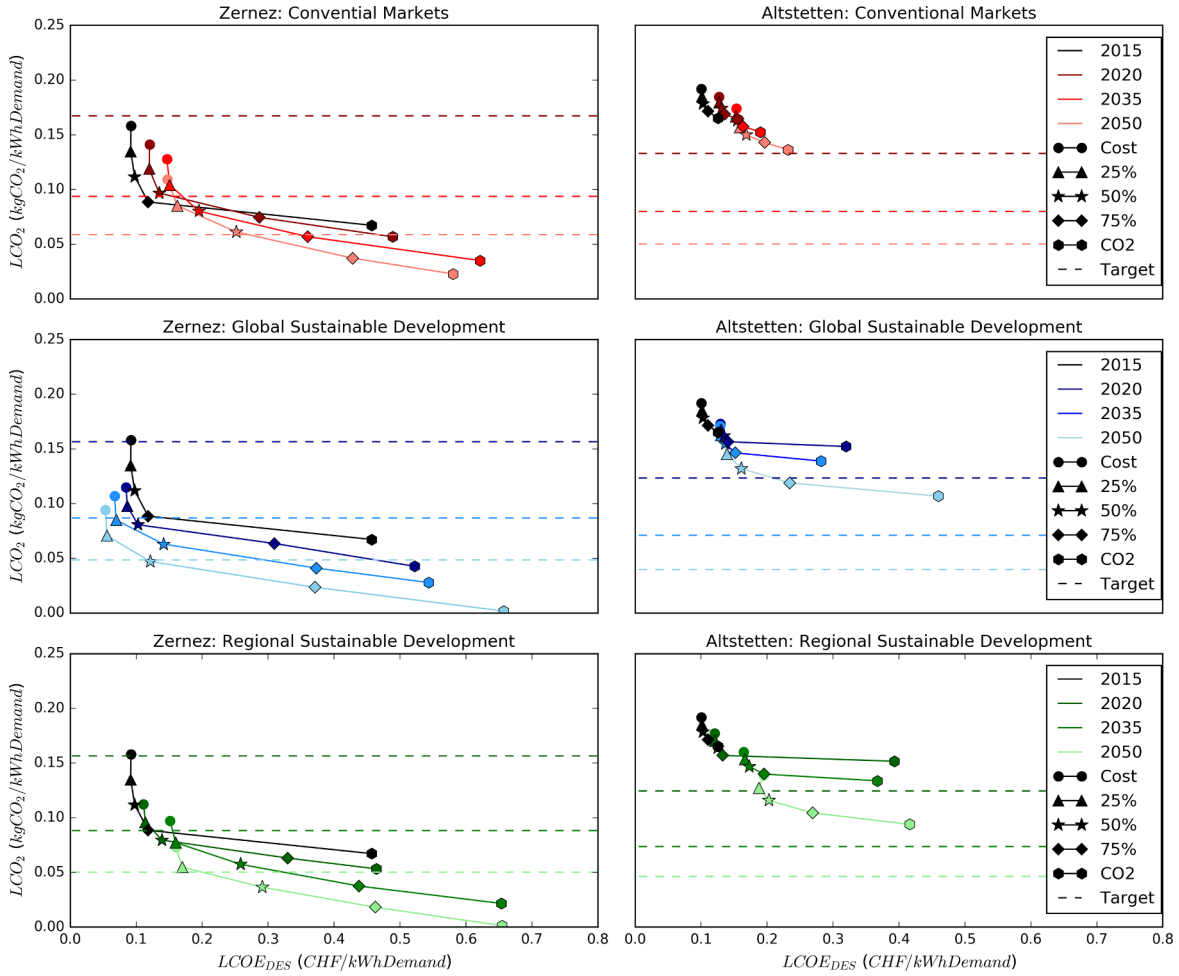

Fig. 7. Pareto fronts for each year and scenario. Dashed lines represent energy targets and colours represent the year.

increase in costs in the CO_2 optimal solution is mostly caused by installation of a large hydrogen storage systems and the capital required to build them. It should be noted that the sizes of these large hydrogen storage systems in the CO_2 optimal solutions are most likely infeasible as it would require too much space for hydrogen storage tanks, however these solutions provide us with reference point to the minimum possible feasible emissions that can be theoretically obtained. Typically solutions at the elbows of these curves would represent the best trade-off of emissions and cost, although ultimately it would be up to a decision maker to decide where along the curve the ideal solution would lie. If the intention is to meet the energy targets, all three future scenarios are projected to be able to meet the energy targets with the 50% CO_2 objective solution in 2050 in Zernez. In Altstetten, all solutions miss the energy strategy targets.

5.2. Performance of the case studies in the context of the Swiss Energy Strategy 2050

In Fig. 8, the results from Fig. 7 have been replotted with respect to the buildings energy density ($\frac{E}{A}$ from Eq. (30)) on the x-axis and the system CO_2 intensity ($\frac{C}{E}$ from Eq. (30)) in order to benchmark the feasible options against the energy targets.

Fig. 8 shows the energy density values decreasing (or energy efficiency of the buildings increasing) in both case studies over time due to the continuous retrofit of buildings. The energy strategy targets are shown in the dashed grey lines for the years of 2020, 2035, and 2050 according to the Kaya identity calculations described in Section 3.3.6. For the Zernez case study, it is seen that the 50% CO_2 minimization objective is able to meet the emissions targets in 2050 in all three future scenarios.

In Altstetten, it is again seen that solutions miss the targets, which implies that solutions that meet targets are infeasible given the energy demand and renewable potentials available. This does not mean that the case study will be unable to meet its targets, but rather it will miss the targets by solely relying on the implementation of the DES concept and the and the presumed retrofit rates. The building stock in Altstetten is comprised of mostly older multi-family houses, resulting in a high heating density. There is also a high ratio of heated and electrified area vs. the available area for solar installations compared to the rural case study. Due to the low renewable potential, there is not enough renewable energy generated on-site to meet the targets. In order to improve the buildings energy performance, a higher retrofit rate should be adopted for the neighbourhood, however even if the retrofit rates are increased, additional renewable energy would most likely still be required to meet the targets due to the shallow slope of the target curves

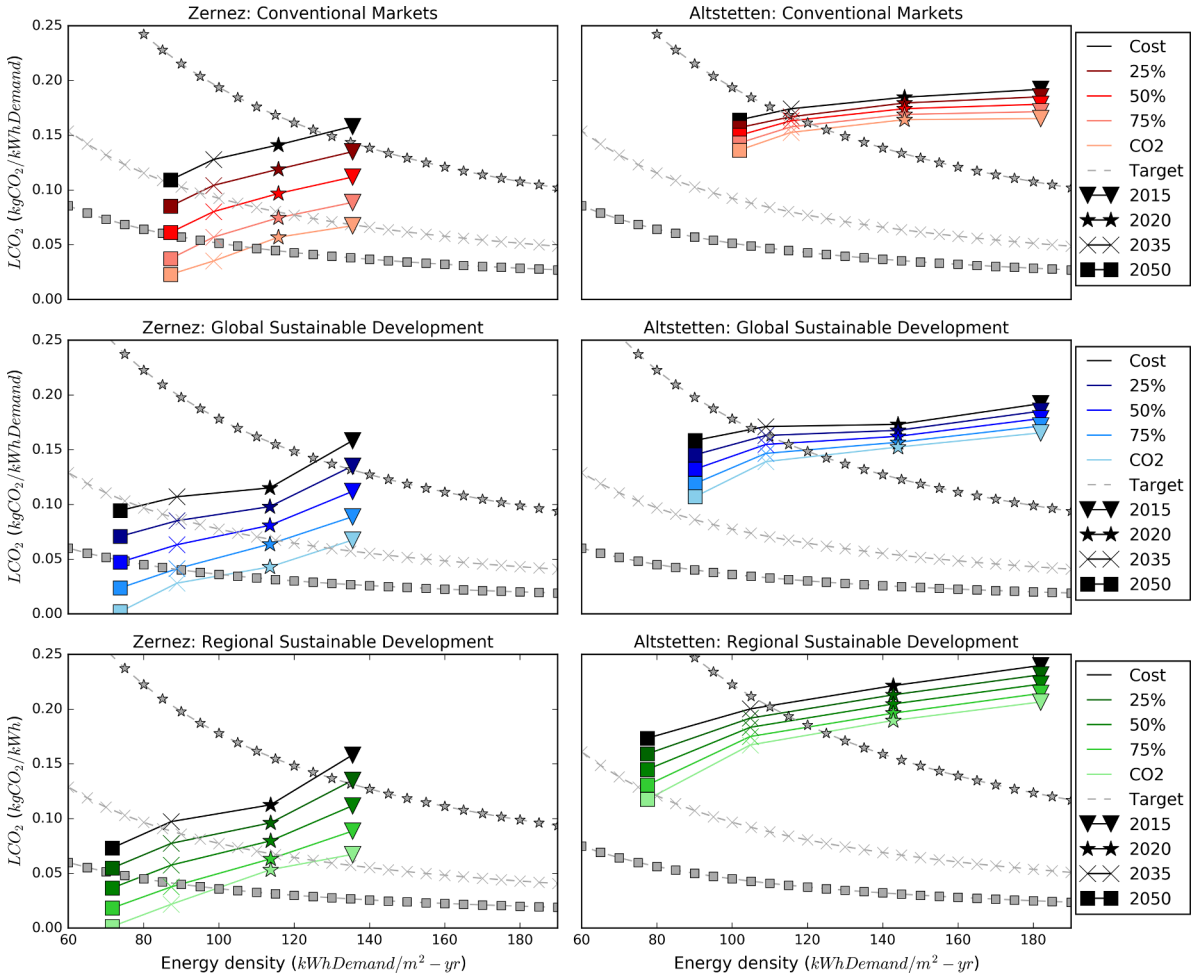

Fig. 8. Building total (electricity and heat) energy density vs. the LCO_2E for all Pareto optimal solutions.

in 2050. Renewable energy imports, such as biomass, biogas, or externally produced PV or wind would need to be imported into the DES in order to meet targets in this neighbourhood.

5.3. Technology sizing

The conversion and storage technology sizing associated with the 50% CO_2 minimization solutions are shown in Fig. 9. The 50% CO_2 minimization objective is shown, as it represents the most cost effective solution that is able to meet the energy strategy targets in 2050 in Zernez in each future scenario. The technologies are separated by conversion technologies (both dispatchable and non-dispatchable) and storage technologies.

Here, RES technologies such as PV and HPs are both cost effective and cost optimal as they are installed in their full capacity in almost all cases. Small-wind is also installed in the same fashion but to a lesser extent due to the high costs and low output of small-wind turbines. MGTs are often installed in the year of 2015 and in many of the CM solutions due to low gas prices, but are not installed when the prices increase in the GSD and RSD scenarios. Boilers are also installed in all cases as they are typically the back-up heating technology that is relied upon. Since heat demand cannot simply be purchased from a central grid in times of need, thermal storage systems and boilers are heavily relied upon due to the high heating demand of both case studies in winter.

PEMFC, H2S, and PEMEC represent technologies that must be installed to implement hydrogen storage systems. The size of hydrogen storage systems increases over time as the technology capital costs become cheaper, the performance of the equipment improves, there is a higher level of surplus energy, and electricity costs increase. In addition, it is seen that the largest H2S systems are installed in the RSD systems, followed by the CM and lastly the GSD. The difference is dependent on the feed-in tariff of the scenarios. The RSD and the CM scenarios both have a quick phase out of the feed-in tariff, while the GSD scenario keeps the feed-in tariff high until 2050. As a result, it is more profitable in the GSD scenario to sell surplus electricity back to the grid rather than storing it on-site. The RSD scenario has the largest hydrogen storage systems, as it has a higher level of surplus electricity than the CM scenario due it its lower demand. With a large amount of surplus electricity available, the system chooses to store this electricity rather than sell it to the grid at a low rate. The results find it is almost always optimal to install RES technologies, as it opts to purchase the maximum feasible amount available for nearly all objectives.

In the Altstetten case study, small hydrogen systems are installed. Due to the lower renewable potential, the system found it is preferable to install batteries and to use hydrogen storage for storage durations longer than one day (although seasonal storage is never used).

5.4. Increase in share of renewables over time

Each of the 100 solutions previously shown not only represents the design of the system configuration and the sizes of the technologies but

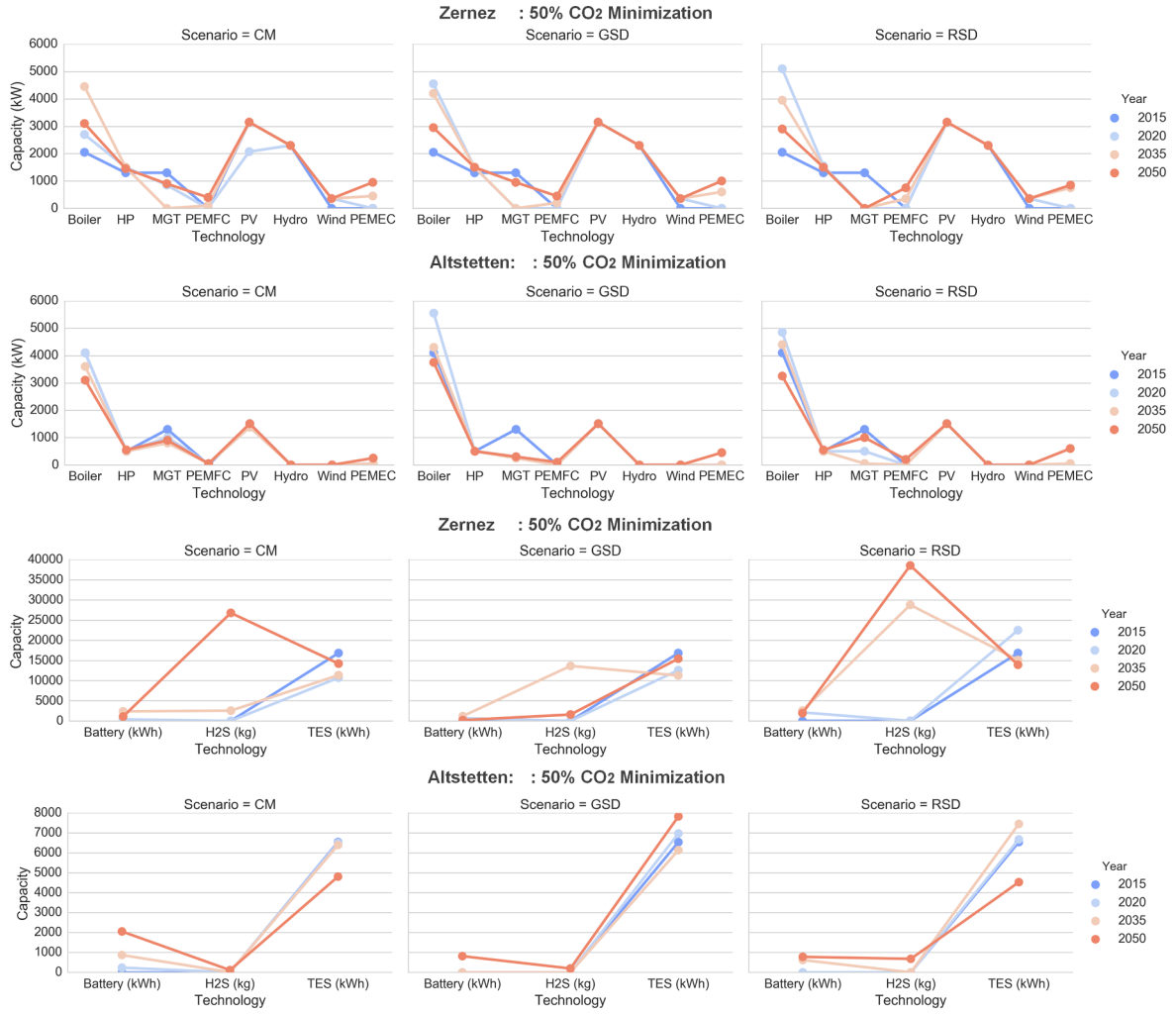

Fig. 9. Conversion (above) and Storage (below) technology sizing for the 50% CO_2 minimization objectives.

also their operation. Fig. 10 shows the technology outputs that contribute to the total annual aggregated demand of the case studies for the years of 2015 to 2050. It is split by the demand carriers of electricity and heating.

Fig. 10 shows that heat pumps, PV, and hydro all contribute greatly to the end energy demand. As the demand decreases over time, the same output from these devices allows boilers, gas turbines, and grid electricity to be used less. Stored energy is used in greater portions in 2050 with PEMFCs and batteries playing an increasing role, especially in the RSD case. Thermal storage is also used, but its potential is already maximized in 2015 and it remains constant until 2050 as its costs begin low and are predicted to remain constant over time. It is to be noted that although the percentages of hydro and PV use in Zernez appear to decrease over time their use is not actually decreasing, but rather more production is being used to charge the storage technologies as opposed to being used directly to meet demand (the future demand is lower due to retrofits). In addition, a higher portion of renewable energy is sold back to the grid, especially in the GSD case. In Altstetten, the demand in 2050 is still dependent on boilers, MGT, and grid electricity due to the lack of renewables.

These figures show that heat pumps and PV play a key role in both case studies. Their total potential is restricted due to available area of installation specific to each case study, but nevertheless they are predicted to be the most cost effective and low carbon technology available for the futures of both case studies for heating and electricity demands respectively. In addition, the RSD scenario has the highest portion of storage usage by 2050. The high feed-in tariffs in the GSD case disincentives storage of renewables on-site and promotes selling electricity back to the grid. This implies that the feed-in tariff does not promote the use of on-site storage systems, and thus does not foster self-sustainability in the local neighbourhood. A high feed-in tariff with a high penetration of RES could cause many producers to sell their electricity back at the same time, resulting in centralized grid overloading issues. The use of on-site storage can prevent these issues by allowing neighbourhoods to store this energy rather than selling it back to the grid. This study therefore recommends a phase out of the feed-in tariff between 2020 and 2030 to incentivize the use of local storage solutions, thus promoting on-site consumption.

5.5. Storage performance

In order to further compare the load shifting with the storage systems in each scenario, Fig. 11 shows the charging and discharging of each of the three storage systems over the full simulation year in 2050 for the 50% CO_2 minimization solution. For hydrogen storage, charging energy is represented by the amount of electricity input into the electrolyser and the discharging energy is accounted for in two streams: hydrogen directly injected into the natural gas grid and energy (both

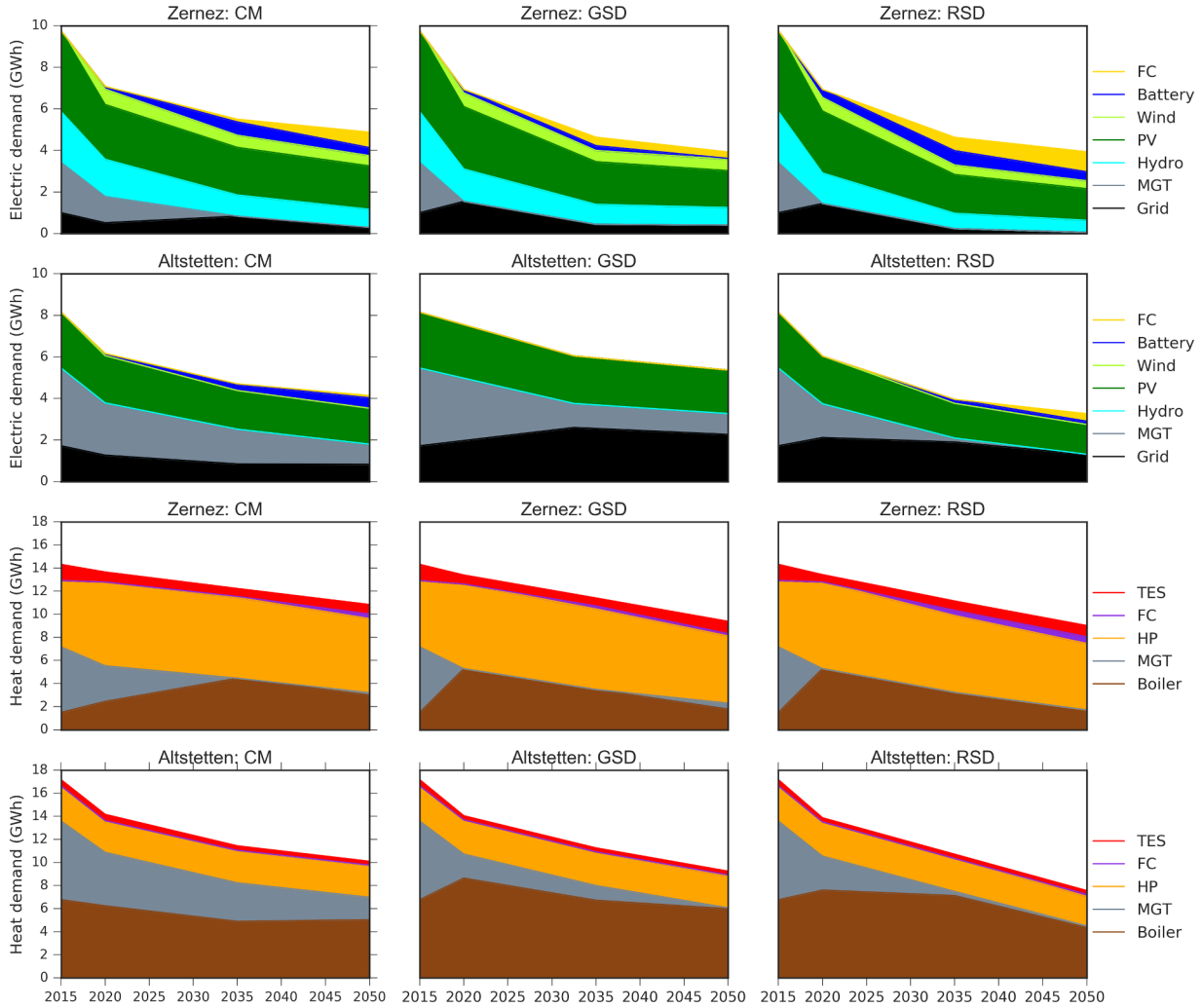

Fig. 10. Energy demand (electricity and heat) met by each energy source from 2015 to 2050 for the 50% CO_2 minimization solutions. Please note that renewable technology output (i.e., PV, wind and hydro) refers to only demand that is directly met from these technologies rather than renewable energy stored in storage systems. Renewable energy from storage systems is shown as energy met from the Battery, TES, and fuel cell (which, although not a storage technology is powered by stored hydrogen gas).

heat and electricity) produced from the PEMFC. Both the battery and thermal storage are also shown with their charging and discharging energy.

In Zernez, the storage systems are used to a larger extent, as there is a higher renewable surplus. Although a P2H system is used in all three future scenarios in Zernez in 2050, it is used the least in the GSD case study due to the high feed-in tariff. In summer, there is only a small amount of heating demand for domestic hot water, and the electricity can be met directly from the hydro and PV resources, therefore the storage is not needed significantly in the short-term and the renewable electricity can be sold back to the grid for profit. In both the CM and RSD scenarios, the behavior of a long-term storage system can be observed as the surplus is used to charge the hydrogen storage predominantly in the summer, as it is no longer profitable to sell the surplus back to the grid due to the phase out of the feed-in tariff. The surplus of hydrogen charged in the summer is then used by the fuel cell in the winter, thus taking advantage of a seasonal shift in energy. In the RSD case, the long-term hydrogen storage is used to a greater extent due to the higher renewable surplus caused by the lower demands.

In Altstetten, the hydrogen system is only used in the summer when there is a renewable surplus and is used to shift energy over a few days at maximum. In the GSD and RSD scenarios, the hydrogen storage is able to shift a similar amount of energy compared to the thermal and battery storages but it does not shift the energy demand from month to month, as was done in Zernez. The CM scenario uses short-term storage more than the hydrogen storage. Due to the lower renewable surplus, short-term storage is preferable to long-term storage as it is more efficient.

When comparing the optimal storage technologies in the two cases, it is clear that hydrogen storage requires a high level of renewable surplus in order to be feasible as a long-term storage. In neighbourhoods where the renewable potential is too low, it will not have enough load to shift for long-term storage to be feasible. In addition, if the feed-in tariff remains high, hydrogen storage is less likely to be used as the profits of selling surplus electricity back to the grid will be higher than the value of stored energy in the hydrogen system. This is observed in the GSD scenario in both case studies, where the surplus electricity is sold to the grid rather than stored in the hydrogen system during the summer's renewable electricity surplus.

6. Conclusion

In this paper, we have developed a methodology to assess the potential of long and short-term storage in future scenarios with a multi-

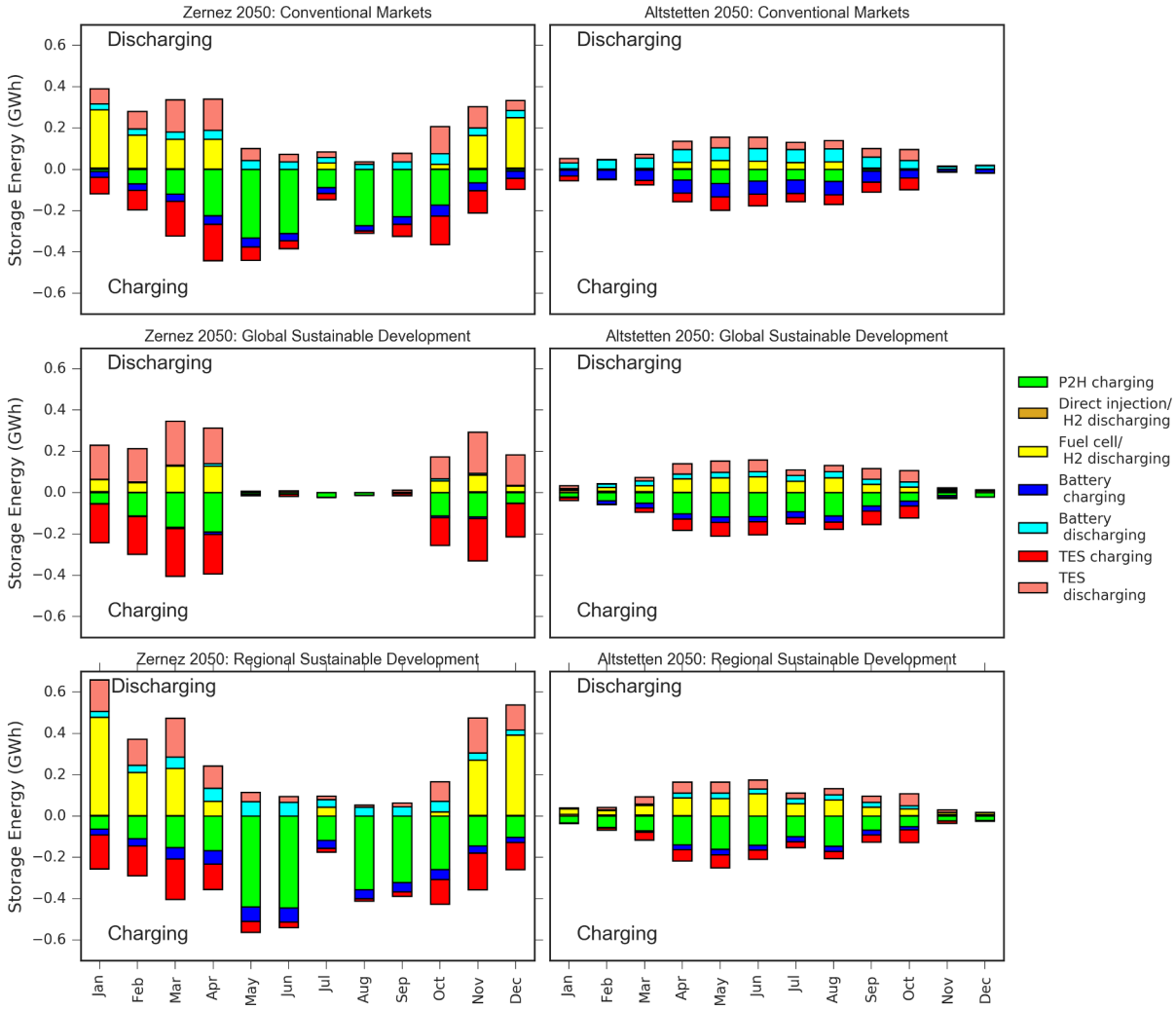

Fig. 11. Charging and discharging of the storage technologies for the 50% CO_2 objective minimization solutions in 2050 for each month in the 2050. Negative values indicate the charging of the storage technologies and positive values indicate the discharging of storage technologies.

objective optimization for DES that evaluates he optimal configurations from 2015 to 2050. The model has a specific emphasis on the evaluation of a decentralized long-term P2H system. In order to properly capture the operation of these technologies, part-load PWA functions are used for the fuel cells and electrolysers and a full year time horizon is used to establish storage continuity over a full year in order to evaluate charge and discharge cycles up to one year in length (seasonal storage). Three future scenarios, framed from the IPCC, Special Report on Emissions Scenarios, were used for evaluation of the future years of 2020, 2035, and 2050. They are titled *Conventional Markets*, representing global markets with a strong economic focus, *Global Sustainable Development* representing global markets with a strong environmental focus, and *Regional Sustainable Development* representing regional markets with a strong environmental focus.

This model can be used for evaluation of any decentralized energy system. It will be able to highlight the technologies that are the most cost effective to decarbonize the building stock and can to determine if the targets will be able to be met from renewable energy produced on-site or whether alternatives (i.e., external renewable energy certificates) will have to be considered to meet national emissions targets. Energy planners tasked with deciding which technologies, systems, or methods will be the most effective and least expensive to meet targets for the buildings in their communities can use such a model to evaluate their own project or community within certain boundaries. Policy makers can use such a model to assess a variety of neighbourhoods to see which technologies they should promote in certain areas and to what extent retrofit rates should be increased.

To demonstrate this, the model was evaluated with two case studies in different settings: one urban and one rural, both with different amounts of renewable potential. Pareto optimal solutions were run for all combinations of future years, future scenarios, and case studies. The solutions are compared against the national future energy strategy targets, which provides valuable information for policy makers and energy planners. In addition, the full-year horizon directly targets the differences between long-term and short-term storage.

Separate conclusions can be made from the findings of the two case studies. For the rural case study (Zernez), the high renewable potential allows for several solutions that were able to meet the energy targets. Due to the high level of renewables, long-term storage was an asset in the design after 2035 when the feed-in tariff was phased out. The urban case study (Altstetten) could not meet the targets in any scenario due to the lack of available renewables and the remaining high level of energy demand due to the older building stock. Although the retrofit rates were the same for both case studies, the higher energy demand of the older building stock in the urban case study would have benefited more from a higher retrofit rate as an energy reduction strategy. Long-term storage

was not feasible in this case as there was not enough renewable surplus to shift with the storage. Instead, short-term storage was sufficient to shift the load for this case study. From this analysis, we can conclude that long-term storage is only attractive for case studies with a sufficiently high level of renewable surplus. In summary, the specific analysis into long-term P2H storage did show that the technology is both technically feasible with sufficient amounts of renewable surplus and that it likely will become more attractive in the future, particularly in case studies where a deep decarbonization is wanted or required.

Aside from the storage systems, it was found that retrofit and renewable energy integration were both required to meet the energy strategy targets. For the neighbourhood with less renewable potential and an old building stock, in this case the urban case study, the importance of retrofits should be particularly emphasized as the targets could not be met. The population density in the urban case study resulted in a lower amount of rooftop space for PV relative to the energy density of the buildings. In an urban area, alternative strategies to solar technologies would be difficult to include due to the lack of available area to install other technologies. To further decrease the use of fossil fuels, external renewable energy must be imported into the neighbourhood (i.e., the community could purchase renewable energy shares or certificates).

The results of the three future scenarios show that storage systems were the most favoured in the RSD scenario. This was due to the lower local demand resulting in higher surplus electricity. Due to low feed-in tariffs and increasing electricity prices, it was more cost effective to install a storage system and use this energy at a later time rather than selling it back to the grid at a low cost. The CM scenario also favoured storage despite having the lowest renewable surplus of all scenarios, which implies that the feed-in tariff has a strong effect on storage system selection and capacity. The GSD scenario was also effective at reducing emissions and was the most cost favourable scenario due to the feed-in tariff profits, however it choose to sell most of its surplus back to the grid which may result in stress on the centralized grid and a lower self-sustainability ratio. All three scenarios were able to meet the emissions reduction targets for the rural case study and its storage systems. This suggests that both long and short-term storage could play an important role in helping DES in settings with large renewable potential meet their energy strategy targets.

When planning for the future, decision makers should also consider the effects that the input parameters have on the optimal system configuration and thus on their ability to contribute to emission reduction targets. Results show that feed-in tariff and the level of surplus energy (which is highly impacted by the building energy demand and the level of available renewable potential) have a high impact on the optimal system design. If the realized parameters for these values in the future vary strongly from the predictions, then the conclusions of this paper will differ. In such a model, uncertainty in the input parameters and their effect on the model must be considered and the effects of these future outcomes should be known before decisions are made regarding the implementation of these systems.

In order to further investigate the impacts of input parameters, an uncertainty analysis and sensitivity analysis of this model parameters should be performed, although the computational time of the model would likely have to be reduced to conduct a proper uncertainty analysis with a Monte Carlo method (typically requiring thousands of runs). More simulations would have to be run on the identified parameters of interest (i.e., feed-in tariff, electricity price, capital cost of storage and RES, and retrofit rate) to draw further conclusions.

These additions would strongly build on the method of multi-objective optimization for DES that is investigated in this paper and would allow for the better identification of energy strategies for decarbonization, which could be a powerful tool to meeting the climate change goals by 2050.

Acknowledgements

This research is part of the ‘Integration of sustainable multi-energy hub systems at the neighbourhood scale from the buildings perspective’ (IMES-BP 407040-153890) and the ‘Economic assessment of multi-energy-hub systems integration at the neighbourhood scale’ (IMES-ECO 407040-153781) projects in the Energy Turnaround NRP70 Research Programme. Funding for this research is provided by the Swiss National Science Foundation (SNF).

The authors would like to thank all IMES project partners, especially Bastien Girod for his contributions for the development of the scenarios. We would also like to thank Paolo Gabrielli for his assistance in setting the parameters for the future scenarios and development of the PWA for the fuel cell and electrolyser.

Appendix A. Future parameters

The parameters used in the optimization are listed in this section. Table A.1 lists the economic and market parameters, Table A.2 lists the technology parameters, and Table A.3 lists the lifetimes of technologies.

Table A.1
Future scenario economic and market parameters.

Parameter	Baseline	CM			GSD			RSD		
	2015	2020	2035	2050	2020	2035	2050	2020	2035	2050
Elec. price (CHF/kWh)	0.198 [52]	0.206 [31]	0.235 [31]	0.231 [31]	0.212 [31]	0.251 [31]	0.262 [31]	0.212 [31]	0.251 [31]	0.262 [31]
Gas price (CHF/kWh)	0.067 [53]	0.037 [32]	0.052 [32]	0.061 [32]	0.095 [32]	0.129 [32]	0.148 [32]	0.193 [32]	0.270 [32]	0.305 [32]
Feed-in tariff (CHF/kWh)	0.176 [6]	0.087 [6]	0 [31]	0 [31]	0.176 [6]	0.176 [6]	0.176 [6]	0.087 [6]	0.011 [31]	0.001 [31]
Grid CO_2 (kg CO2/kWh)	0.124 [54]	0.150 [54]	0.150 [54]	0.150 [54]	0.100 [54]	0.089 [54]	0.072 [54]	0.100 [54]	0.089 [54]	0.074 [54]
CO_2 tax (CHF/t CO2)	84 [55]	84 [55]	84 [55]	84 [55]	120 [55]	240 [55]	240 [55]	120 [55]	240 [55]	240 [55]
Discount rate (%)	6.0 [56]	6.0 [56]	6.0 [56]	6.0 [56]	6.0 [56]	6.0 [56]	6.0 [56]	6.0 [56]	6.0 [56]	6.0 [56]
Retrofit rate (%)	1.0 [31]	1.0 [31]	1.0 [31]	2.0 [31]	2.0 [31]	2.0 [31]	2.0 [31]	2.0 [31]	2.0 [31]	2.0 [31]

Table A.2
Future scenario technology parameters.

Technology	Parameter	Baseline	CM			GSD			RSD		
		2015	2020	2035	2050	2020	2035	2050	2020	2035	2050
PV	Capital Cost (CHF/m2)	334 [57]	334 [57]	334 [57]	334 [57]	225 [58]	136 [58]	124 [58]	225 [58]	136 [58]	124 [58]
	OMV cost (CHF/kWh)	0.034 [58]	0.034 [58]	0.034 [58]	0.034 [58]	0.025 [58]	0.014 [58]	0.012 [58]	0.025 [58]	0.014 [58]	0.012 [58]
	Nominal efficiency	17.0% [59]	17.0% [59]	17.0% [59]	17.0% [59]	17.0% [59]	17.0% [59]	17.0% [59]	17.0% [59]	17.0% [59]	17% [59]
Small-hydro	Capital Cost (CHF/kW)	3478 [60]	3478 [60]	3478 [60]	3478 [60]	3478 [60]	3478 [60]	3478 [60]	3478 [60]	3478 [60]	3478 [60]
	OMF cost (CHF/kW)	104 [60]	104 [60]	104 [60]	104 [60]	104 [60]	104 [60]	104 [60]	104 [60]	104 [60]	104 [60]
	Nominal efficiency	80% [38]	80% [38]	80% [38]	80% [38]	80% [38]	80% [38]	80% [38]	80% [38]	80% [38]	80% [38]
[]-3exSmall-wind	Capital Cost (CHF/kW)	9200 [58]	9200 [58]	9200 [58]	9200 [58]	8674 [58]	8477 [58]	8017 [58]	8674 [58]	8477 [58]	8017 [58]
	OMV cost (CHF/kWh)	0.014 [58]	0.014 [58]	0.014 [58]	0.014 [58]	0.014 [58]	0.014 [58]	0.014 [58]	0.014 [58]	0.014 [58]	0.014 [58]
Heat pump	Capital Cost (CHF/kW)	1977 [57]	1977 [57]	1977 [57]	1977 [57]	1600 [58]	1500 [58]	1400 [58]	1600 [58]	1500 [58]	1400 [58]
	OMF cost (CHF/kW)	5.4 [58]	5.4 [58]	5.4 [58]	5.4 [58]	4.4 [58]	4.1 [58]	3.9 [58]	4.4 [58]	4.1 [58]	3.9 [58]
	Nominal COP	3.2 [41]	3.2 [41]	3.2 [41]	3.2 [41]	3.2 [41]	3.2 [41]	3.2 [41]	3.2 [41]	3.2 [41]	3.2 [41]
Gas boiler	Capital Cost (CHF/kW)	260 [57]	260 [57]	260 [57]	260 [57]	260 [57]	260 [57]	260 [57]	260 [57]	260 [57]	260 [57]
	OMF cost (CHF/kW)	3.7 [57]	3.7 [57]	3.7 [57]	3.7 [57]	3.7 [57]	3.7 [57]	3.7 [57]	3.7 [57]	3.7 [57]	3.7 [57]
	Nominal efficiency	85% [58]	85% [58]	85% [58]	85% [58]	85% [58]	85% [58]	85% [58]	85% [58]	85% [58]	85% [58]
PEMFC	Capital Cost (CHF/kW)	6252 [5]	2886 [5]	1443 [5]	962 [5]	2886 [5]	1443 [5]	962 [5]	2886 [5]	1443 [5]	962 [5]
	OMV cost (CHF/kWh)	0.025 [61]	0.025 [61]	0.025 [61]	0.025 [61]	0.025 [61]	0.025 [61]	0.025 [61]	0.025 [61]	0.025 [61]	0.025 [61]
	Nom. Elec. efficiency	50% [62]	55% [63]	58% [27]	60% [64]	55% [63]	58% [27]	60% [64]	55% [63]	58% [27]	60% [64]
	Thermal efficiency	48% [62]	43% [63]	37% [27]	35% [64]	43% [63]	37% [27]	35% [64]	43% [63]	37% [27]	35% [64]
[]-8exMGT	Capital Cost (CHF/kW)	900 [65]	750 [65]	620 [65]	500 [65]	750 [65]	620 [65]	500 [65]	750 [65]	620 [65]	500 [65]
	OMV cost (CHF/kWh)	0.013 [65]	0.013 [65]	0.013 [65]	0.013 [65]	0.013 [65]	0.013 [65]	0.013 [65]	0.013 [65]	0.013 [65]	0.013 [65]
	Nom. Elec. efficiency	25% [65]	28% [65]	30% [65]	32% [65]	28% [65]	30% [65]	32% [65]	28% [65]	30% [65]	32% [65]
	Thermal efficiency	70% [65]	70% [65]	70% [65]	70% [65]	70% [65]	70% [65]	70% [65]	70% [65]	70% [65]	70% [65]
[]-3exPEMEC	Capital Cost (CHF/kW)	2650 [5]	2200 [5]	1500 [5]	760 [5]	2200 [5]	1500 [5]	760 [5]	2200 [5]	1500 [5]	760 [5]
	OMF cost (%Cap)	5% [66]	5% [66]	5% [66]	5% [66]	5% [66]	5% [66]	5% [66]	5% [66]	5% [66]	5% [66]
	Nominal Efficiency (kWh/Nm3)	6.00 [5]	5.5 [5]	5 [5]	4.5 [5]	5.5 [5]	5 [5]	4.5 [5]	5.5 [5]	5 [5]	4.5 [5]
Li-ion Battery	Capital Cost (CHF/kWh)	674 [67]	578 [67]	482 [67]	385 [67]	260 [67]	260 [67]	260 [67]	260 [67]	260 [67]	260 [67]
	OMF cost (CHF/kWh)	25 [68]	25 [68]	25 [68]	25 [68]	25 [68]	25 [68]	25 [68]	25 [68]	25 [68]	25 [68]
	Overall efficiency	92.5% [2]	92.5% [2]	92.5% [2]	92.5% [2]	92.5% [2]	92.5% [2]	92.5% [2]	92.5% [2]	92.5% [2]	92.5% [2]
[]-3exThermal storage	Capital Cost (CHF/m^3)	650 [57]	650 [57]	650 [57]	650 [57]	650 [57]	650 [57]	650 [57]	650 [57]	650 [57]	650 [57]
	Overall efficiency	90% [43]	90% [43]	90% [43]	90% [43]	90% [43]	90% [43]	90% [43]	90% [43]	90% [43]	90% [43]
Hydrogen Storage	Capital Cost (CHF/kgH2)	950 [61]	680 [5]	510 [5]	460 [5]	680 [5]	510 [5]	460 [5]	680 [5]	510 [5]	460 [5]

Table A.3
Future scenario technology lifetimes.

Technology	PV	Small-hydro	Small-wind	Heat pump	Gas boiler	PEMFC	MGT	PEMEC	Li-ion Bat	TES	H2S
Lifetime (years)	25 [69]	50 [60]	25 [58]	20 [58]	20 [58]	–	–	–	11.5 [2]	17 [43]	22 [61]
Operating hrs	–	–	–	–	–	60,000 [5]	30,000 [65]	60,000 [5]	–	–	–

Appendix B. Cost breakdown

The costs displayed in Fig. 7 are further broken down into five categories in Fig. B.1: conversion technology capital, storage technology capital, operation and maintenance, fuel, and electricity costs. The GSD scenario achieves the lowest cost solutions, while the CM scenario has the highest costs. In the cost optimal solutions for the Zernez case study, there are observed negative electricity costs (profits). This is also true for the 25% and 50% solutions for the in the GSD scenario. These are all cases with a high feed-in tariff. In cost optimal solutions, the capital costs of storage and the conversion technologies are responsible for the majority of the costs. This is due to large hydrogen storage systems being installed. More reasonably sized systems are installed in the 50% and 75% cases. In Altstetten, the costs are dominated by natural gas as the case study is strongly dependent on gas boilers to meet its heating demand.

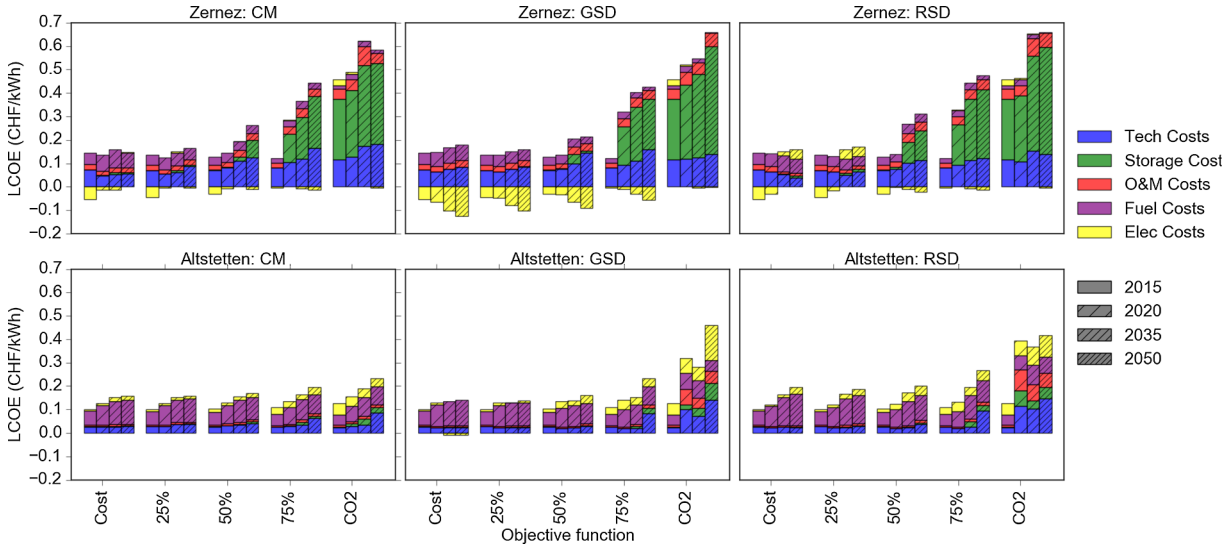

Fig. B.1. Cost objective composition for Pareto optimal solutions.

Appendix C. Supplementary material

Supplementary data associated with this article can be found, in the online version, at https://doi.org/10.1016/j.apenergy.2018.08.106.

References

[1] Parag Y, Sovacool BK. Electricity market design for the prosumer era. Nat Energy 2016;4.
[2] Battke Benedikt, Schmidt Tobias S, Grosspietsch David, Hoffmann Volker H. A review of probabilistic model of lifecycle costs and stationary batteries in multiple applications. Renew Sustain Energy Rev 2013;25:240–50.
[3] Beaudin Marc, Zareipour Hamidreza, Schellenberglabe Anthony, Rosehart William. Energy storage for mitigating the variability of renewable electricity sources: An updated review. Energy Sustain Dev 2010;14(4):302–14.
[4] Götz Manuel, Lefebvre Jonathan, Mrs Friedemann, Koch Amy McDaniel, Graf Frank, Bajohr Siegfried, et al. Renewable power-to-gas: a technological and economic review. Renew Energy 2016;85:1371–90.
[5] Körner Alexander, Tam Cecelia, Benett Simon, Gagné Jean-Francois. Hydrogen technology roadmap - hydrogen and fuel cells. Technical Report, International Energy Agency; 2015.
[6] SwissGrid, KEV-EIV Vergtüngssätze gültig für neue Bescheide; 2015. <http://www.swissolar.ch/topthemen/kev-und-eiv/>.
[7] Nakicenovic N, Swart R. Special Report on Emissions Scenarios, Technical report, Cambridge University Press, Intergovernmental Panel on Climate Change; 2000.
[8] Geidl Martin, Andersson Göran. Operational and structural optimization of multi-carrier energy systems. In: Future power systems conference 2005, vol. 16(5); 2006, pp. 463–477.
[9] Hajimiragha A, Canizares C, Fowler M, Andersson G. Optimal energy flow of integrated energy systems with hydrogen economy considerations. In: iREP Symposium- Bulk Power System Dynamics and Control - VII, Revitalizing Operational Reliability; 2007.
[10] Maroufmashat Azadeh, Fowler Michael, Sattari Sourena, Elkamel Ali, Roshandel Ramin, Hajimiragha Amir. Mixed integer linear programing based approach for optimal planning and operation of a smart urban energy networkto support the hydrogen economy. Int J Hydrogen Energy 2016;41(19):7700–16.
[11] Zhang Yang, Campana Pietro Elia, Lundblad Anders, Yan Jinyue. Comparative study of hydrogen storage and battery storage in grid connected photovoltaic system: Storage sizing and rule-based operation. Appl Energy 2017;201(Supplement C):397–411.
[12] Bernal-Agustín José L, Dufo-López Rodolfo. Techno-economical optimization of the production of hydrogen from PV-Wind systems connected to the electrical grid. Renew Energy 2010;35(4):747–58.
[13] Korpas M, Holen AT. Operation planning of hydrogen storage connected to wind power operating in a power market. IEEE Trans Energy Convers 2006;21(3):742–9.
[14] Petruschke Philipp, Gasparovic Goran, Voll Philip, Krajai Goran, Dui Neven, Bardow Andr. A hybrid approach for the efficient synthesis of renewable energy systems. Appl Energy 2014;135:625–33.
[15] Li Bei, Roche Robin, Paire Damien, Miraoui Abdellatif. Sizing of a stand-alone microgrid considering electric power, cooling/heating, hydrogen loads and hydrogen storage degradation. Appl Energy 2017;205(Supplement C):1244–59.
[16] Dufo-López Rodolfo, Bernal-Agustín José L. Multi-objective design of PV wind

diesel hydrogen battery systems. Renew Energy 2008;33(12):2559–72.
[17] Yang Hongming, Xiong Tonglin, Qiu Jing, Qiu Duo, Dong Zhao Yang. Optimal operation of DES/CCHP based regional multi-energy prosumer with demand response. Appl Energy 2016;167:353–65.
[18] Fazlollahi Samira. Decomposition optimization strategy for the design and operation of district energy system. PhD Thesis, École Polytechnique Fédérale de Lausanne; 2014.
[19] Marquant Julien F, Evins Ralph, Carmeliet Jan. Reducing computation time with a rolling horizon approach applied to a MILP formulation of multiple urban energy hub system. Proc Comput Sci 2015;51:2137–46.
[20] Lunz Benedikt, Stöcker Philipp, Eckstein Sascha, Nebel Arjuna, Samadi Sascha, Erlach Berit, et al. Scenario-based comparative assessment of potential future electricity systems A new methodological approach using Germany in 2050 as an example. Appl Energy 2016;171(Supplement C):555–80.
[21] Simoes Sofia, Nijs Wouter, Ruiz Pablo, Sgobbi Alessandra, Radu Daniella, Bloat Pelin, et al. The JRC-EU-TIMES model - assessing the long-term role of the set plan energy technologies. Eur - scientific and technical research reports, Publications Office of the European Union; 2013.
[22] Sgobbi Alessandra, Nijs Wouter, Miglio Rocco De, Chiodi Alessandro, Gargiulo Maurizio, Thiel Christian. How far away is hydrogen? its role in the medium and long-term decarbonisation of the european energy system. Int J Hydrogen Energy 2016;41(1):19–35.
[23] Han Seulki, Won Wangyun, Kim Jiyong. Scenario-based approach for design and comparatively analysis of conventional and renewable energy systems. Energy 2017;129(Supplement C):86–100.
[24] Ren Hongbo, Gao Weijun. A MILP model for integrated plan and evaluation of distributed energy systems. Appl Energy 2010;87(3):1001–14.
[25] Yazdanie Mashael, Densing Martin, Wokaun Alexander. Cost optimal urban energy systems planning in the context of national energy policies: a case study for the city of Basel. Energy Policy 2017;110(Supplement C):176–90.
[26] McKenna Russell, Merkel Erik, Fichtner Wolf. Energy autonomy in residential buildings: a techno-economic model-based analysis of the scale effects. Appl Energy 2017;189(Supplement C):800–15.
[27] Dodds Paul E, Staffell Iain, Hawkes Adam D, Li Francis, Grnewald Philipp, McDowall Will, et al. Hydrogen and fuel cell technologies for heating: a review. Inter J Hydrogen Energy 2015;40(5):2065–83.
[28] Moss RH, Edmonds JA, Kibbard KA, Manning MR, Rose SK, Van Vuuren DP, et al. The next generation of scenarios for climate change research and assessment. Nature 2010;463:747–56.
[29] Girod Bastien, Wiek Arnim, Mieg Harald, Hulme Mike. The evolution of the IPCC's emissions scenarios. Environ Sci Policy 2009;12(2):103–18.
[30] van Vuuren Detlef P, Kok Marcel TJ, Girod Bastien, Lucas Paul L, Vries Bert de. Scenarios in global environmental assessments: key characteristics and lessons for future use. Glob Environ Change 2012;22(4):884–95.
[31] Prognos AG, Erläuternder Bericht zur Energiestrategie 2050. Technical report, Bundesamt für Energie; 2013. <www.energiestrategie2050.ch>.
[32] U.S. Energy Information Administration (EIA), Annual Energy Outlook 2015 with projections to 2040. Washington, Technical report, U.S. Department of Energy (DOE), Washington; 2015.
[33] Wang Danhong, Landolt Jonas, Mavromatidis Georgios, Orehounig Kristina, Carmeliet Jan. CESAR: a bottom-up housing stock model for Switzerland to address sustainable energy transformation strategies'. Energy Build 2018;129:9–26.
[34] Bundesamt für Statistik, Statistisches Lexikon der Schweiz. GWS/GWR; 2012. <https://www.bfs.admin.ch/bfs/de/home.html>.
[35] Swisstopo. Federal Office of Topography, swissBUILDINGS3d 2.0, 2014. <https://shop.swisstopo.admin.ch/en/>.
[36] Mavromatidis Georgios, Orehounig Kristina, Carmeliet Jan. Evaluation of photovoltaic integration potential in a village. Sol Energy 2015;121:152–68.
[37] Aventa AG, LoWind turbine AV-7; 2016. <http://aventa.ch/en/leichtwindanlage-av-7.html>.
[38] Paish Oliver. Small hydro power: technology and current status. Renew Sustain Energy Rev 2002;6(6):537–56.
[39] Gabrielli P, Flamm B, Eichler A, Gazzani M, Lygeros J, Mazzotti M. Modeling for optimal operation of PEM fuel cells and electrolyzers. In: 2016 IEEE 16th international conference on environment and electrical engineering (EEEIC); 2016, pp. 1–7.
[40] Capstone Turbine Corporation, Products: Capstone Turbine Corporation (CPST); 2017. <https://www.capstoneturbine.com/products/>.
[41] Burkhard Sanner, Current status of ground source heat pumps in europe. In: Current status of ground source heat pumps in Europe, Warsaw, Poland, Justus-Liebig-University, 2003.
[42] Miglani Somil, Orehounig Kristina, Carmeliet Jan. Assessment of the ground source heat potential at the building level applied to a large urban case study. In: Brenet Status-Seminar; 2016.
[43] Stadler Michael, Aki Hirohisa, Firestone Ryan, Lai Judy, Marnay Chris, Siddiqui Afzal. Distributed energy resources on-site optimization for commercial buildings with electric and thermal storage technologies. Technical report, Lawerence Berkeley National Labs, Berkeley, CA, May 2008.
[44] Keirstead James, Samsatli Nouri, Shah Nilay, Weber Cline. The impact of CHP (combined heat and power) planning restrictions on the efficiency of urban energy systems. Energy 2012;41(1):93–103.
[45] Weber C, Shah N. Optimisation based design of a district energy system for an eco-town in the United Kingdom. Energy 2011;36(2):1292–308.
[46] Altfeld Klaus, Pinchbeck Dave. Admissible hydrogen concentration in natural gas systems. Technical report, The European Gas Research Group; 2013.
[47] Carl Knopf F. Modeling, Analysis and optimization of process and energy systems John Wiley & Sons; 2011.
[48] Laumanns Marco, Thiele Lothar, Zitzler Eckart. An adaptive scheme to generate the pareto front based on the epsilon-constraint method. In: Practical approaches to multi-objective optimization, dagstuhl seminar proceedings. Internationales Begegnungs- und Forschungszentrum fr Informatik (IBFI), Schloss Dagstuhl, Germany; 2005.
[49] Mavromatidis Georgios, Orehounig Kristina, Richner Peter, Carmeliet Jan. A strategy for reducing co2 emissions from buildings with the Kaya identity A Swiss energy system analysis and a case study. Energy Policy 2016;88(Supplement C):343–54.
[50] Orehounig Kristina, Mavromatidis Georgios, Evins Ralph, Dorer Viktor, Carmeliet Jan. Towards an energy sustainable community: an energy system analysis for a village in switzerland. Energy Build 2014;84:277–86.
[51] Remund J, Müller SC, Schilter C, Rihm B. The use of meteonorm weather generator for climate change studies. In: 10th EMS Annual Meeting, 10th European conference on applications of meteorology (ECAM), September 2010, pp. EMS2010–417.
[52] Eidgenössische Elektrizitätskommission, Strompreis, 2017. <https://www.strompreis.elcom.admin.ch/>.
[53] Bildung und Forschung WBF Eidgenössisches Department für Wirtschaft, Der website des preisüberwachers zu den gaspreisen, 2015. <http://gaspreise.preisueberwacher.ch/web/index.asp>.
[54] Itten Rene, Frischknecht Rolf, Stucki Matthias. Life cycle inventories of electricity mixes and grid, resreport, Paul Scherrer Institut (PSI); 2014.
[55] Pierre-Alain Bruchez, Auswirkungen eines Klima- und Energielenkungssystems für 2030: Analyse mit einem berechenbaren Gleichgewichtsmodell für die Schweiz, Technical report, Ecoplan AG; 2015.
[56] Northwest Power and Conservation Council, Sixth northwest conservation and electric power plan, techreport, Northwest Power and Conservation Council; 2010.
[57] Jakob Martin, Kallio Sonja, Nägeli Claudio. Intergrated strategies and policy instruments for retrofitting buildings to reduce primary energy use and GHG emissions (INSPIRE). <http://www.energieschweiz.ch/de-ch/wohnen/energierechner/inspire-tool.aspx>.
[58] Centre for Climate and Energy Economics, Technology data for energy plants, techreport, Danish Energy Agency; 2016.
[59] Lang Tillmann, Gloerfeld Tillmann, Girod Bastien. Don't just follow the sun a global assessment of economic performance for residential building photovoltaics. Renew Sustain Energy Rev 2015;42(Supplement C):932–51.
[60] International Energy Agency. Renewable energy essentials: Hydropower, Technical report, International Energy Agency; 2010.
[61] Amos Wade A. Costs of storing and transporting hydrogen. National renewable energy laboratory; 1998. <https://www.nrel.gov/docs/fy99osti/25106.pdf>.
[62] Wang Caisheng, Nehrir MH, Shaw SR. Dynamic models and model validation for PEM fuel cells using electrical circuits. IEEE Trans Energy Convers 2005;20(2):442–51.
[63] Tsuchiya Haruki, Kobayashi Osamu. Mass production cost of PEM fuel cell by learning curve. Int J Hydrogen Energy 2004;29(10):985–90.
[64] Schoots K, Kramer GJ, van der Zwaan BCC. Technology learning for fuel cells: an assessment of past and potential cost reductions. Energy Policy 2010;38(6):2887–97.
[65] do Nascimento Marco Antônio Rosa, de Oliveira Rodrigues Lucilene, dos Santos Eraldo Cruz, Gomes Eli Eber Batista, Dias Fagner Luis Goulart, Velásques Elkin Iván Gutirrez, et al. Micro gas turbine engine: a review. Chapter 5 in Progress in Gas Turbines; 2013.
[66] Lehner Marcus, Tichler Robert, Steinmller Horst, Koppe Markus. Power-to-Gas: Technology and Business Models, Springer; 2014.
[67] Lott Melissa, Kim Sang-Il, Tam Cecillia, Technology Roadmap - Energy Storage, techreport, International Energy Agency, 2014. <https://www.iea.org/publications/freepublications/publication/TechnologyRoadmapEnergystorage.pdf>.
[68] Rastler D. Electricity energy storage technology options: a white paper primer on applications, costs, and benefits, Technical Report 1020676, Electric Power Research Institute; 2010.
[69] Jordan Dirk C, Kurtz Sarah R. Photovoltaic degradation rates - an analytical review. Technical report, National Renewable Energy Laboratory; 2012.